Neuroscience

Diverging roles of TRPV1 and TRPM2 in warm-temperature detection

Muad Y. Abd El Hay, **Gretel B. Kamm**, **Alejandro Tlaie**, **Jan Siemens**

Department of Pharmacology, Heidelberg University, Heidelberg, Germany • Ernst Strüngmann Institute for Neuroscience in cooperation with the Max Planck Society, Frankfurt am Main, 60528, Germany • Laboratory for Clinical Neuroscience, Centre for Biomedical Technology, Technical University of Madrid, Spain

Reviewed Preprint

Published from the original preprint after peer review and assessment by eLife.

About eLife's process

Reviewed preprint version 1
March 5, 2024 (this version)

Sent for peer review
December 28, 2023

Posted to preprint server
December 18, 2023

Abstract

The accurate perception of innocuous temperatures, particularly those experienced as pleasantly warm, is essential for achieving thermal comfort and maintaining thermoregulatory balance. Warm-sensitive neurons (WSN) innervating the skin play a central role in non-painful warmth detection. The TRP ion channels TRPV1 and TRPM2 have been suggested as sensors of warm temperature in WSNs. However, the precise contribution of these channels to the process of warmth detection is not fully understood.

A significant challenge in analysing WSNs lies in their scarcity: fewer than 10 % of sensory neurons in the rodent dorsal root ganglion (DRG) respond to innocuous warm temperatures. In this study, we examined >20,000 cultured mouse DRG neurons using calcium imaging and discovered distinct contributions of TRPV1 and TRPM2 to warm-temperature sensitivity. TRPV1 and TRPM2 affect the abundance of WSNs, with TRPV1 mediating the rapid, dynamic response to warmth.

By carefully tracking animal movement in a whole-body thermal preference paradigm, we observe that these cellular differences correlate with nuanced thermal behaviours. Utilizing a driftdiffusion model to quantitatively analyse the decision-making process of animals exposed to different environmental temperatures, we found that: TRPV1 primarily impairs the precision of evidence accumulation, whereas TRPM2 significantly increases the total duration of exposure to uncomfortably warm environments.

Our findings provide valuable insights into the distinct molecular responses to warmth stimuli, and underpin the subtle aspects of thermal decision-making when encountering minor temperature variations.

eLife assessment

In this **important** manuscript, Abd El Hay and colleagues reveal a clear role of TRPV1 and TRPM2 receptors in warm temperature perception and present a technically unique experimental strategy to measure and analyze temperature preference behavior, which will have a lasting impact on the field. In addition to the behavioral data, which is strong, the study provides an analysis of cultured sensory neurons to controlled warmth stimuli - in this case, the evidence relating the activity of TRPM2 channels to the behavioral responses of animals is **incomplete**. Overall, the findings are of importance for neuroscientists, physiologists, and biophysicists, as there is still substantial discussion in the field regarding the contribution of TRP channels to different aspects of thermosensation.

Introduction

The detection of temperature, and the related behavioural responses, are an integral part of our sensory interaction with the outside world. Thus, it is not surprising that temperature detection was one of the first sensory modalities to be studied in contemporary neuroscience (1). Early studies concentrated on the characterization of temperature-specific sensory fibres, covering the range from noxious cold, through innocuous cold and warm, to noxious heat (2). However, the molecular mechanism by which temperature activates these fibres remained elusive for decades.

A major breakthrough in the field of somatosensory research was the identification of temperature-sensitive ion channels that belong to the transient-receptor potential (TRP) super family as the molecular sensors responsible for the detection of noxious cold and heat in sensory neurons (3–5). However, the temperatures in-between noxious cold and heat (25 °C to 43 °C), which are often perceived as non-painful, received less attention. This innocuous temperature range also contains the so-called thermoneutral point (TNP); an ambient temperature (29 °C to 33 °C) at which mice do not exert additional energy to maintain their body temperature (6). This makes the innocuous temperature range crucial for thermoregulation and the animal's subsequent thermal or comfort choice. Recent studies began to uncover the mechanisms behind innocuous warm-temperature detection, thereby mainly converging on two candidate cation channels, namely TRPV1 and TRPM2 (7–10). Interestingly, the evidence for the involvement of both channels is seemingly contradictory.

TRPV1 is traditionally associated with the response to noxious temperature stimuli (> 42 °C), with the ability to become sensitive to lower temperatures in inflammatory contexts (3, 11–13). However, *in vivo* calcium imaging of trigeminal sensory neurons in animals lacking TRPV1 showed a complete absence of responses to warm stimuli applied to the oral cavity of mice, while responses to hot temperatures were unchanged. Furthermore, acute inhibition of TRPV1 in animals trained to discriminate innocuous cold from warmth through a nose port led to a reduction in their performance (7). These results stand in contrast to other studies that showed no involvement of TRPV1 in warm-temperature detection, neither in thermal preference assays nor in an operant behaviour task with stimuli applied to the paws (14–17).

TRPM2 has reported *ex vivo* activation temperatures between 35 °C and 40 °C, depending on the cellular context, and was first described as a physiological temperature sensor in pancreatic islet cells (18, 19). Calcium imaging of DRG cultures from animals lacking TRPM2 showed a reduction in the proportion of warm- and heat-responsive neurons in comparison to wildtype sensory neuron cultures (8). Interestingly, *Trpm2*$^{-/-}$ animals are unable to differentiate

temperatures across the innocuous warm range in thermal preference tasks (8, 20), while their ability to avoid noxious temperatures is not affected. However, this result is challenged by the minor deficits observed in the *Trpm2*-deficient animals trained to report warming of their paws (17).

In summary, both for TRPV1 and TRPM2, there is an apparent disconnect between the observations in cellular assays and the behavioural tasks assessing temperature detection. *In vivo* calcium imaging coupled with warm-temperature stimuli only shows a relevance of TRPV1, but not TRPM2 in the innocuous temperature range (7). Contrary to that, the lack of TRPM2, but not TRPV1, more consistently affects warm-temperature detection in assays of temperature preference (8, 14–16), but not for operant behavioural assays (7, 17).

One main challenge for the analysis of WSNs, neurons that respond to innocuous temperature stimuli between 25 °C and 43 °C, is the low abundance of this neuronal population, which represents about 3 % to 10 % of sensory neurons in rodents (8, 21). Using in-depth functional analysis of 1000s of sensory neurons from multiple animals, we here describe that TRPV1 and TRPM2 are both involved in the detection of innocuous (warm) temperature stimuli. Furthermore, we demonstrate the diverging roles both channels play in warm-temperature detection through a novel thermal preference behaviour assay.

Results

The thermal chamber preference test allows precise discrimination of subtle temperature differences in the innocuous range

Mice prefer 31 °C to warmer temperatures when ambient and floor temperature are controlled

The ability to avoid uncomfortable environmental temperatures or move toward pleasant thermal conditions is fundamental to sustaining life. This process is known as behavioural thermoregulation and can be found in most groups of animals (22). The preference of rodents for temperature is traditionally assessed via paradigms that challenge the animals with differing floor temperatures (23–25). This leads to preference development that is based on temperature detection through glabrous skin, such as the paws, tail, and nose. Animals, however, are capable of integrating temperature from glabrous and non-glabrous skin (26). With the aim to probe behavioural thermoregulation in a more holistic context, we developed a thermal discrimination assay where both the floor and ambient temperature are controlled, termed the thermal chamber preference test (CPT) (**Figure 1A-D**, **Figure S1**). When presented with warm ambient temperatures (34 °C and 38 °C) and 31 °C as control temperature, mice significantly preferred the 31 °C chamber over the warmer chambers (**Figure 1E** and **F**, Table S2). Compared to the classic two-plate preference test (TPT), wildtype animals developed a stronger preference for the 31 °C side in the CPT (**Figure S1I**). Additionally, animals showed a clear preference for 31 °C when given 34 °C as an option in the CPT. This is not observed in the classic TPT (**Figure S1I**). This observation suggests that more subtle ambient temperature differences, relating to comfort and thermoregulation, are more faithfully assessed in the CPT assay.

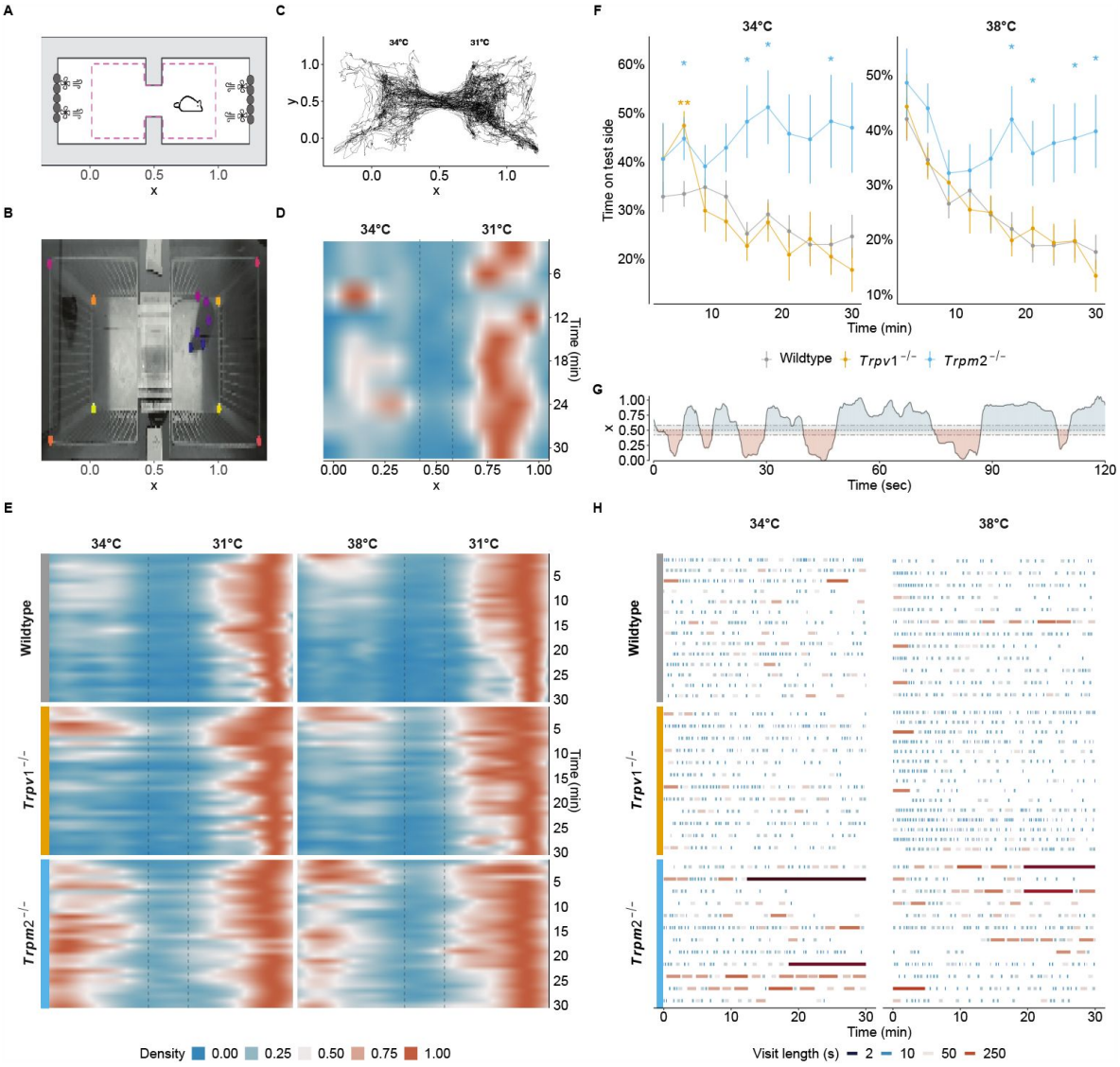

Fig. 1.

A novel ambient temperature preference test.

A Schematic of the chamber preference test from the top. Grey outlines the outer enclosure and the dashed line the internal cage. Peltier elements (grey oval shapes) were combined with fans for precise control of the temperature. See Figure S1 for a more detailed view. **B** A representative image of an animal exploring the chambers. Coloured dots represent the tracked keypoints on the animal and reference points in the enclosure. **C** Tracking of an example animal for 30 minutes at 31 °C (right chamber) and 34 °C (left chamber). **D** Density maps of the x-position of the animal in **C** over 30 minutes; binned in three-minute long intervals, concatenated, and interpolated. Dashed lines represent the tunnel connecting both chambers. **E** Density maps as in **D** with one-minute bins of all animals from wildtype (n = 48), *Trpv1*$^{-/-}$ (n = 15) and *Trpm2*$^{-/-}$ (n = 28) genotypes. **F** Proportion of time spent in the test chamber for animals shown in **E** over time, binned in three-minute long intervals. * (p <0.05), ** (p <0.01). See Table S2 for statistical details. **G** Exemplary behaviour of the animal in **C** and **D** over the first 120 seconds of the experiment, highlighting the visit frequency and duration of time spent in each chamber. The dashed line represents the tunnel connecting the chambers. **H** Overview of the frequency and length of the visits to the test chamber for 15 randomly sampled animals per genotype, shown in **E**. Each visit is coloured by the log2 of its length to highlight varying visit lengths.

TRPM2 is necessary for establishing a preference in the warm-temperature range

Previous studies assessing warmtemperature detection using the TPT with animals lacking TRPV1 or TRPM2 showed that *Trpm2*$^{-/-}$ animals failed to differentiate between 31 °C and 38 °C while *Trpv1*$^{-/-}$ animals, similar to wildtypes, preferred the 31 °C side (15, 27). Similarly, when using the newly developed CPT, *Trpv1*$^{-/-}$ animals showed a similar temperature preference to wildtypes while *Trpm2*$^{-/-}$ animals failed to develop a preference for the thermoneutral (31 °C) side (**Figure 1E-F**), without affecting their preference at 25 °C (**Figure S2A-B**). In addition to the previously described phenotype at 38 °C, *Trpm2*$^{-/-}$ animals were also unable to discriminate 34 °C from 31 °C, emphasizing the relevance of TRPM2 at milder warm temperatures (**Figure 1E-F**, and **Figure S1**). Notably, the phenotype of *Trpm2*$^{-/-}$ animals was similar to that of animals lacking most, if not all, peripheral (heat and cold) thermosensors (*Trpv1*^{Abl}, (28), **Figure S1J-L**). These results confirm previous data demonstrating the requirement for TRPM2 rather than TRPV1, in preference development in the warm-temperature range (8, 15).

TRPV1 and TRPM2 affect different aspects of warm-temperature detection

Traditionally, analyses of temperature preference are limited to reporting the proportion of time an animal spent at the test temperature, without assessing more finegrained thermal preference behaviour, such as the sequence of chamber crossings and intermittent pauses (visit lengths, (23–25)). We observed that in the CPT, animals cross from one chamber to the other, probing the chamber, before crossing back (**Figure 1G**). We quantified the number of crossings and the lengths of these episodes throughout the experiments (**Figure 1H**). At the start of the experiment, mice of all genotypes crossed more often than at the end of the experiment while maintaining similar durations of their visits to the warmer chamber (**Figure 1H**, **Figure S1C-D**). *Trpv1*$^{-/-}$ animals showed a significantly higher crossing rate compared to wildtype animals at both 34 °C and 38 °C (Table S2). *Trpm2*$^{-/-}$ animals, on the other hand, had significantly longer visits to the warmer chamber compared to wildtype animals, while having either similar (at 38 °C) or a reduced crossing rate (at 34 °C) (**Figure 1H**, Table S2).

Notably, animals lacking TRPM8, a cold-sensitive TRP-channel that was shown to be critical for reporting warming in an operant behavioural assay (17), showed similar behaviour to wildtype animals across the warm-temperature range, but deficits at 25 °C (**Figure S2F-G** and Table S2).

Together, these observations suggest that, contrary to previous findings using the TPT, both TRPV1 and TRPM2 contribute to the animals' ability to detect warm temperatures and to drive associated thermal preference behaviours, albeit through different mechanisms.

Trpv1 and *Trpm2* knockouts have decreased proportions of WSNs

A small subpopulation of cultured primary sensory neurons responds to warm temperatures

Trpv1 and *Trpm2* are highly expressed in peripheral sensory neurons that reside bilaterally in so-called dorsal root ganglia (DRG) along the spinal cord. To assess the individual contribution of both channels to ambient warm-temperature detection, and to account for the integration of temperature across the whole body of the animal, we cultured primary DRG neurons pooled from across the whole length of the spine.

Historically, experiments studying temperature responses in sensory neurons are performed with DRG neurons cultured for a few hours to overnight (29). However, these cultures did not reflect the distribution of WSNs described from *in vivo* studies, with 26 ± 9 % of all cells responding to

warm temperatures, contrary to 3 % to 10 % of WSNs observed *in vivo* (**Figure S3A-C**, (7, 21)). We speculated that this expansion in the proportion of WSNs might reflect a post-injury state in which heat-sensitive neurons become sensitised to lower thermal stimuli (7, 30). Since sensory neuron dissociation resembles an axotomy which activates injury-related pathways (31–36), we extended the commonly used DRG primary culture protocol to three days, to allow the cells to recover from the procedure. Three-day cultures harboured approximately 6 ± 3 % WSNs, compared to overnight culture's 26 ± 9 % (**Figure S3C**). Furthermore, three-day cultures showed a reduced calcium inflow upon stimulation, and an improved capacity to return to baseline calcium levels upon termination of the stimulus, counteracting hallmarks of post-injury states of sensory neurons (**Figure 2D** and **Figure S3D-E**, (33, 34)). These observations are in line with data collected from *in vivo* calcium imaging preparations of both dorsal root and trigeminal ganglion cells in response to warm temperatures (7, 21) and suggest that three-day cultures – rather than acute/short-term preparations – more accurately reflect the functional properties and abundance of warm-responsive sensory neurons that are found in behaving animals.

Trpv1 and Trpm2 deletion reduces the proportion of warmth responders

To investigate the effects of TRPV1 and TRPM2 loss on the response of sensory neurons to warm-temperature stimulation, we applied the same stimulation protocol to cultures from *Trpv1*$^{-/-}$ and *Trpm2*$^{-/-}$ animals. Lack of TRPV1 or TRPM2 led to a significant reduction in the proportion of WSNs, compared to wildtype cultures (**Figure 2D**, Table S2). Cultures from *Trpv1*$^{-/-}$ animals had reduced proportions of responders across the whole range of warm-temperature stimuli (**Figure 2B** and D), but showed similar proportions of heat responders (neurons responding to $T \geq 43$ °C) when compared to cultures obtained from wildtype animals (**Figure S3J**). In contrast to a previous study describing WSNs *in vivo* (7), our *Trpv1*$^{-/-}$ cultures did not show a complete absence of response to warm temperatures, with some cells in the *Trpv1*$^{-/-}$ cultures retaining their ability to respond to warm stimuli (**Figure 2B** and D). Lack of TRPM2, on the other hand, affected the proportions of responders across both the warm and the hot temperature range (**Figure 2D** and **Figure S3J**). This is the first cellular evidence for the involvement of TRPM2 on the response of DRG sensory neurons to warm-temperature stimuli, given that previous studies had only assessed noxious/painful heat responses ($T \geq 45$ °C (8)).

WSNs vary in their response characteristics

Consistent with the behavioural data (**Figure 1**), the absence of TRPV1 or TRPM2 led to deficits in the response to warm temperatures in primary sensory neurons. However, how these cellular deficits contribute to the difference in behavioural phenotypes was still unclear. A closer look at the calcium response profiles showed that cells vary in when, and how, they respond to temperature stimuli (**Figure 2B** and **Figure 3B**). To capture this variability, we computed the point at which each cell started responding to the stimulus (**Figure 3B**).

TRPV1 drives the dynamic phase of a warm-temperature response

Each temperature stimulus has two distinct phases: an initial, dynamic phase, in which the temperature rises rapidly. And a second, static phase, in which the temperature stabilizes (**Figure 3C**). The majority of WSNs from wildtype animals respond during the rising, dynamic phase of the stimulus (**Figure 3D** and **E**). In comparison, WSNs from animals lacking TRPV1 predominantly responded during the static phase of the stimulus, while *Trpm2*$^{-/-}$ cells did not significantly differ in their response onset from wildtype cells (**Figure 3D** and **E** and **Figure S4A-C**). Additionally, TRPV1-positive cells in wildtype cultures – identified by their response to the TRPV1 activator capsaicin (3) – predominantly responded during the dynamic phase of the stimulus, compared to TRPV1-negative cells (**Figure S4D-F**). Collectively, these observations suggest that TRPV1, but not TRPM2, is involved in the response to dynamic, fast changes in temperature.

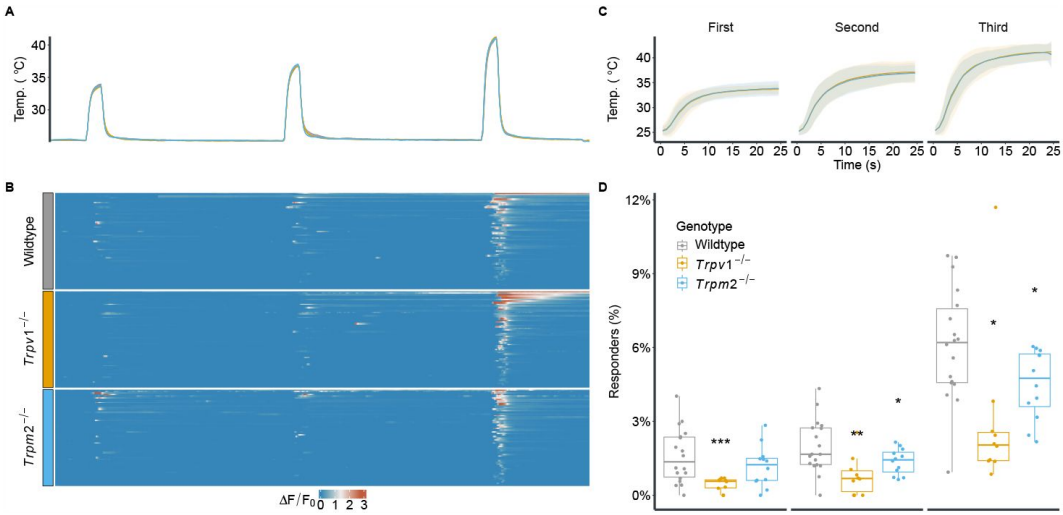

Fig. 2.

Loss of TRPV1 or TRPM2 leads to a reduction in WSN abundance.

A Experimental paradigm of temperature stimulation. Three sequential and increasing temperature stimuli of 25 seconds, with 5 minute inter-stimulus intervals. Traces represent mean temperatures for wildtype, *Trpv1*$^{-/-}$, and *Trpm2*$^{-/-}$ cultures. **B** Heat map showing representative normalized ($\Delta F/F_0$) calcium response of WSNs (60 randomly sampled cells per genotype). **C** Zoom-in of the mean and standard deviation of the three warm-temperature stimuli shown in A. **D** The proportions of responders to each stimulus in relation to all imaged neurons from wildtype (7 animals, 21 FOVs, 6928 cells), *Trpv1*$^{-/-}$ (5 animals, 17 FOVs, 5410 cells), and *Trpm2*$^{-/-}$ (6 animals, 18 FOVs, 6131 cells). Each dot represents a field of view (FOV). * ($p < 0.05$), ** ($p < 0.01$), *** ($p < 0.001$). See Table S2 for statistical details.

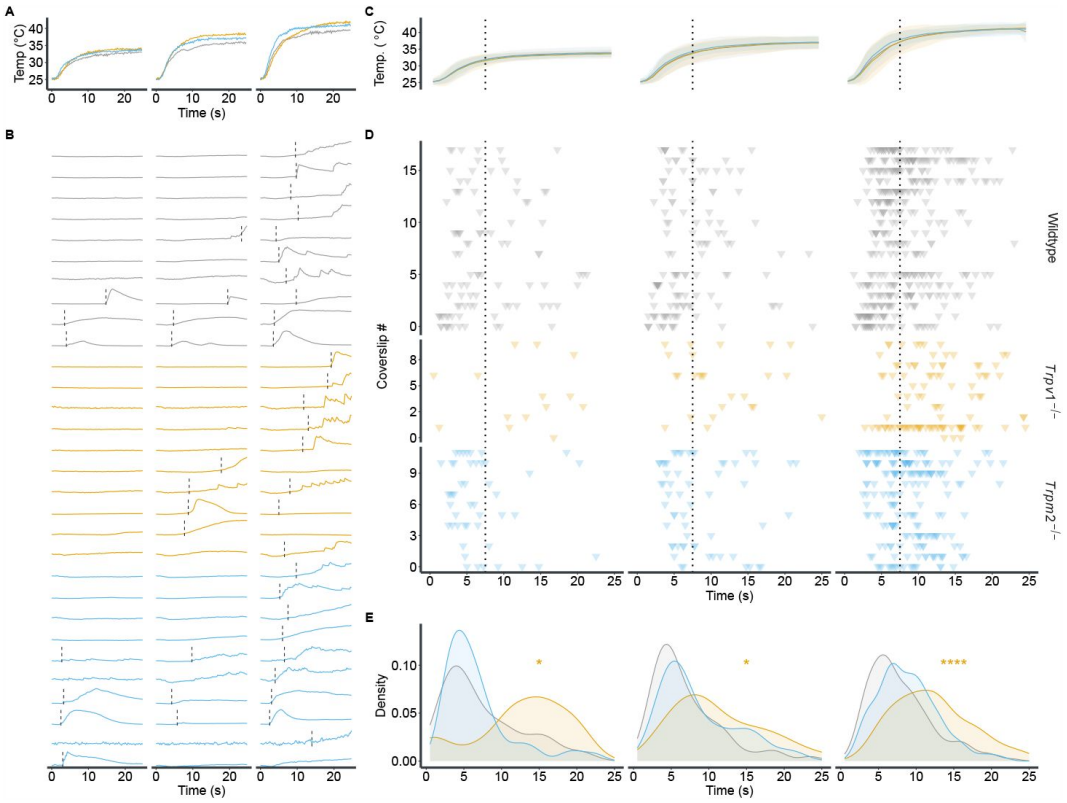

Fig. 3.

Trpv1$^{-/-}$ diminishes the response to dynamic temperature changes.

A Temperature traces from three exemplary imaging sessions. **B** Individual calcium traces ($\Delta F/F_0$) of 10 representative thermosensitive neurons from each genotype in response to the applied stimuli. The position of the dashed line indicates the time when the cells exceeded 10 % of their maximum $\Delta F/F_0$ during the stimulus. **C** Mean and standard deviation of the three warm-temperature stimuli shown in **A**. The dotted line indicates the separation between the dynamic and static phases, defined by the end of the peak of the smoothed temperature change rate. **D** Response onset of all recorded WSNs. Each row represents a single FOV (see **Figure 2D**). Each triangle indicates the time point at which the individual cell responds to the stimulus as shown in **B**. Dotted line as in **C. E** Density plot of response time points for each genotype and stimulus. * ($p < 0.05$), **** ($p < 0.0001$). See Table S2 for statistical details.

Given the strong modulation of the intracellular calcium dynamics observed in *Trpv1*$^{-/-}$ DRGs exposed to warm stimuli, we speculate that over-expression of *Trpv1* would alter the response dynamics of WSNs, particularly during the rising phase of the stimulus. To test this hypothesis, we made use of a previously described animal model which over-expresses *Trpv1* in TRPV1-positive cells (*Trpv1*^{OX}, (37)). WSNs from *Trpv1*^{OX} animals showed a significantly higher propensity to respond during the dynamic phase of the stimulus, when compared to wildtype cultures (**Figure 4A-E**, Table S2). These results align with our previous observations and further suggest that TRPV1 abundance directly regulates the onset and speed of a temperature response.

Does the enrichment of cells responding during the dynamic stimulus phase affect the behaviour of the animals in the CPT? Indeed, *Trpv1* over-expression led to a significantly stronger avoidance of warm temperatures in the CPT (**Figure 4F** and **G**, Table S2). Interestingly, *Trpv1*^{OX} animals crossed significantly less between chambers, compared to wildtype animals, while having similar duration of stays at the test chamber (**Figure 4H**, Table S2), suggesting that *Trpv1*^{OX} animals discriminate temperatures more rapidly.

An evidence-accumulation model uncovers differences in evidence accumulation across genotypes

In the previous sections, we have detailed the distinct effects that TRPV1 and TRPM2 exert on the temperature responses of sensory neurons. While these cellular-level findings are illuminating, they present a challenge when it comes to directly relating them to the more complex, multifaceted behaviours observed in our temperature preference assay. To bridge this gap, we conceptualized the temperature preference assay as a continuous decision-making process (**Figure 5A** and **Figure 5B**), allowing the use of established evidence accumulation frameworks. These models have been shown to successfully recapitulate animal and human behaviour in sensory decision tasks involving different modalities (38–40) and have even been directly linked to neural observations (41, 42).

In our experimental setup, an animal enters a chamber and begins to accumulate evidence (i.e., it continuously collects and computes spatial temperature information) that drives its decision to stay or leave the chamber (**Figure 5A**). The resulting time spent in each chamber varies from visit to visit (**Figure 1G** and **Figure 5A**), highlighting the need to account for a dynamic decision-making process. Crucially, temperature perception is not static; this is particularly evident at the beginning of each visit, when the temperature difference is most pronounced, and changes over time until a threshold is reached that causes the animal to leave (**Figure S1H**). Traditional approaches to analysing these behaviours have largely overlooked these nuances, focusing instead on final outcomes or mean stay time (8, 15, 43), without considering the fluctuating nature of sensory perception and the variability of decision-making across visits and between individual animals.

A drift diffusion model recapitulates the animals' behaviour in the CPT

To model this decision-making process, we opted for a drift diffusion model (DDM (44)). This model provides a quantitative framework to delve into how animals integrate sensory information over time, leading to their decision to stay or leave a chamber (**Figure 5**).

When an animal enters a chamber, it starts at a certain point (z) from which the evidence accumulation begins (**Figure 5B**). Over time, and while the temperature information is integrated, the evidence is accumulated at a certain rate (drift rate, v) and noise level (sv), which represents the variability in evidence accumulation. This process evolves until the decision bound (a) is reached, which prompts the animal to leave the chamber. **Figures 5C** and **D** show simulations of the DDM, which allow an intuition into how varying levels of drift and noise (while keeping the starting point and decision bound fixed) alters the distribution of visit lengths

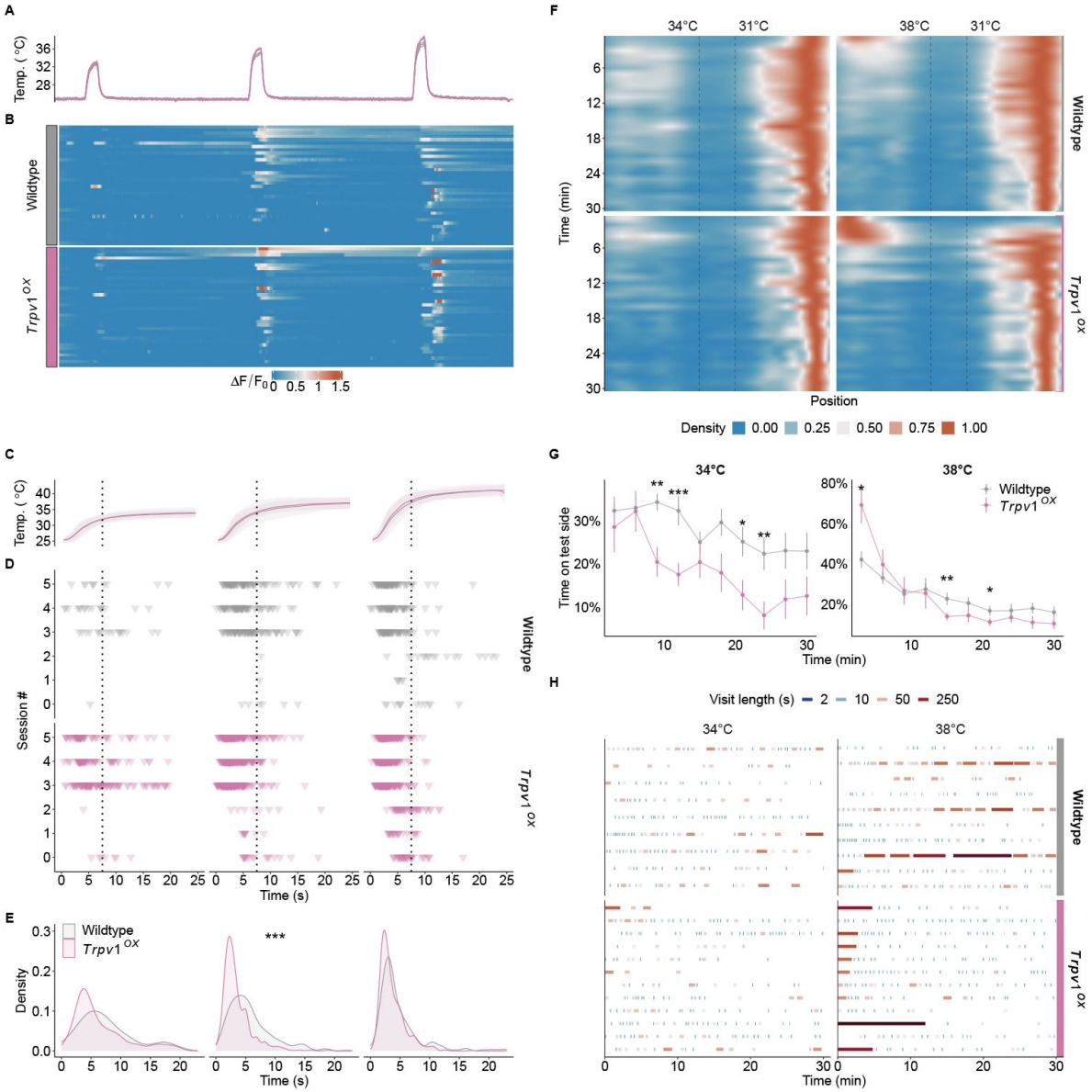

Fig. 4.

High TRPV1 expression levels promote dynamic warm-temperature detection and enhance temperature preference.

A Mean temperatures from all experiments and imaging sessions for wildtype (3 animals, 6 FOVs, 3133 cells) and *Trpv1*^{OX} (2 animals, 5 FOVs, 3754 cells) cultures. **B** Examples of normalized ($\Delta F/F_0$) calcium responses of WSNs responding to any of the stimuli depicted in **A**. 42 randomly sampled cells from each genotype. **C** Mean and standard deviation of the three warm-temperature stimuli applied. The dotted line indicates the separation between the dynamic phase and the static phase (see **Figure 3C**). **D** Response initiation of all WSNs imaged from wildtype and *Trpv1*^{OX} animals. Each row represents an individual imaging session. Each triangle denotes the time point at which the cell responds to the stimulus, as shown in **Figure 3B**. Dotted line as in **C. E** Density representation of response time points for each genotype and stimulus.**F** Density maps of all wildtype (n = 48) and *Trpv1*^{OX} (n = 12) animals in the CPT over time. **G** Proportion of time spent in the test chamber for animals shown in **F** over time, binned in 3-minute intervals. **H** Overview of the frequency and length of the visits to the test chamber for all animals shown in **F**. Each visit is coloured by the log2 of its length to highlight varying visit lengths. * (p <0.05), ** (p <0.01), *** (p <0.001). See Table S2 for statistical details.

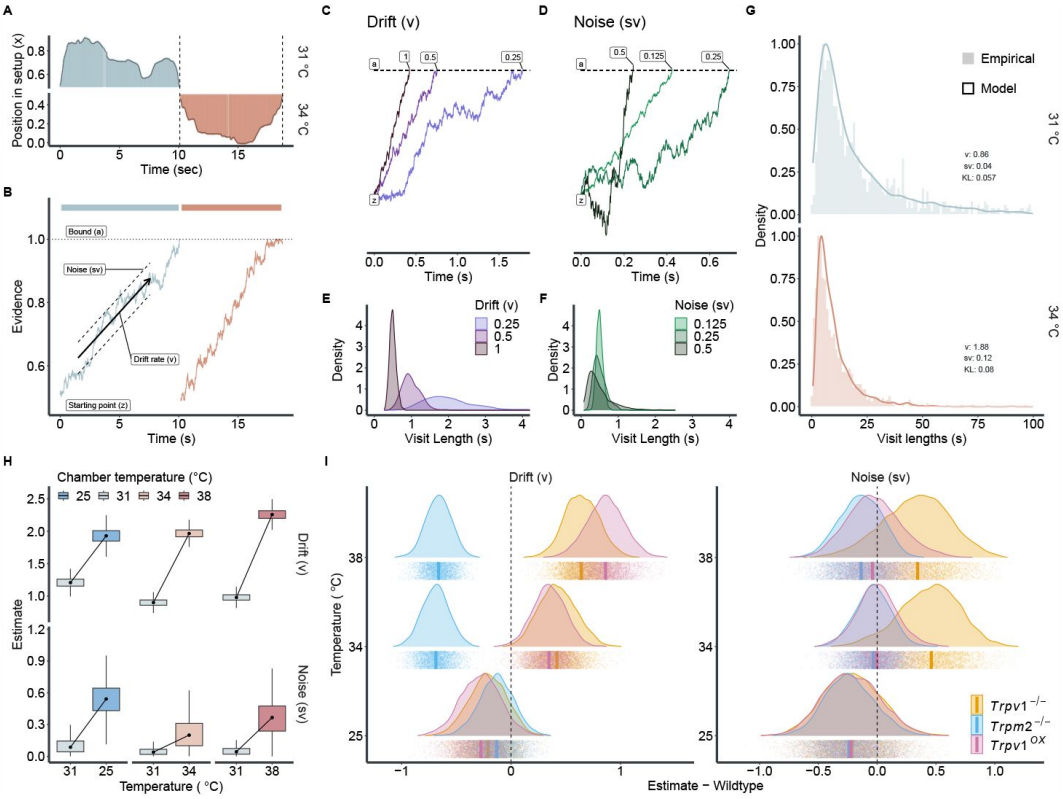

Fig. 5.

Modelling the varying roles of TRPV1 and TRPM2 on warm-temperature detection.

A Two example episodes of an animal inside the CPT, crossing from one chamber to the other (see **Figure 1G**). Dashed line represents crossing time points between chambers. **B** Examples of possible evidence accumulation process for the two episodes in **A** using a Drift Diffusion Model (DDM). **C and D** Simulations of a drift diffusion process with fixed starting points (z = 0.5) and bound (a = 1) while varying drift rates (v in **C**) and noise (sv in **D**). **E and F** depict the resulting distributions of visit lengths when simulating 1000 trials with the parameters from **C** and **D**, respectively. **G** Distributions of visit lengths at 31 °C vs. 34 °C in wildtype animals. Insets show the estimated parameters for v and sv at each temperature and the Kullback-Leibler (KL) divergence between the model (continuous density line) and the empirical data (histogram). See Figure S5 for all model fits. **H** Drift *v* and noise *sv* estimates for both neutral (31 °C, solid line) and test (25 °C to 38 °C, dashed line) chambers for wildtype animals resulting from hierarchical Markov chain Monte Carlo (MCMC) sampling. **I** Neutral chamber (31 °C) corrected and wildtype-subtracted estimates of drift and noise for all genotypes. The dashed line represents the wildtype reference. Points indicate individual MCMC samples, and vertical lines the median of each distribution.

throughout an experiment (**Figures 5E** and **F**). Higher rates of drift (with fixed noise levels) led to overall shorter visit lengths (**Figure 5E**). High noise levels (with fixed drift rates) also led to shorter visit lengths, albeit with larger variability (**Figure 5F**).

We fit a model with varying drift rate and noise onto the visit length distributions of wildtype animals recorded for each temperature combination in the CPT (**Figure 5G** and **Figure S5**). The model suggests higher drift rates at temperatures below and above 31 °C in wildtype animals (**Figure 5H**). Notably, the drift rates in the corresponding neutral chambers (31 °C) are lower than in the test chambers. Both observations are in line with the development of preference for the 31 °C chamber in the varying temperature conditions. The model also suggests an increase in noise in the test temperatures, hinting that the evidence accumulation at 31 °C is particularly stable (**Figure 5H**).

Varying effects of TRPM2 and TRPV1 on evidence accumulation

We fit the model onto all behavioural data collected in this study (**Figure 5I** and **Figure S5**). For animals lacking TRPM2, the model yields a lower drift rate at 34 °C and 38 °C compared to wildtypes (**Figure 5I**). This suggests that loss of TRPM2 leads to a slower evidence accumulation at warm temperatures, reflecting an overall failure to develop a preference for 31 °C throughout the experiment (**Figure 1**). In *Trpv1*$^{-/-}$ animals, on the other hand, we observed higher drift rates as well as higher noise levels in the warmer (34 °C and 38 °C) chambers. These findings suggest that *Trpv1*$^{-/-}$ animals accumulate environmental temperature evidence faster than wildtype animals, but the fidelity of the thermal inputs is compromised. We speculate that the balance of these two variables might lead to a similar overall preference development compared to wildtype animals (**Figure 1**). Interestingly, the over-expression of TRPV1 also leads to an increased drift rate at warm temperatures, albeit with a similar noise level to wildtypes. This combination leads to greater avoidance of 34 °C and 38 °C (as observed in **Figure 4**).

Notably, all genotypes show similar drift and noise estimates at 25 °C, consistent with their behavioural preference (**Figure S2**, suggesting that TRPV1 and TRPM2 mainly control responses to warm temperatures (**Figure 5I**). In summary, we find that the DDM successfully parametrizes the behavioural data obtained from the CPT. Furthermore, the model allowed a more in-depth insight into how the loss of either TRPV1 or TRPM2 differentially alters the detection of warm temperatures, highlighting their importance in behavioural adaptation to innocuous temperatures.

Discussion

Environmental temperatures are detected by sensory nerve fibres innervating the skin. The mechanisms behind warmtemperature detection have recently gained increased attention, with two ion channels, TRPV1 and TRPM2, as the main candidates. In this study, we developed a novel temperature preference assay, integrating ambient and floor temperatures, to investigate the roles of TRPV1 and TRPM2 in temperature detection. Our results reveal distinct behavioural responses to warm temperatures mediated by these channels. Applying a modelling framework to the animal's behaviour, we observed unique deficits in TRPV1 and TRPM2 knockout animals, compared to wildtype mice. On the cellular level, the loss of either TRPV1 or TRPM2 resulted in a decreased proportion of WSNs, with TRPV1 playing a pivotal role in detecting rapid, dynamic temperature changes.

Behavioural analysis in temperature preference assays

The introduced chamber preference assay, integrating both ambient and floor temperatures, improves on the conventional temperature preference assays. Notably, at 34 °C, a temperature that is close to the thermoneutral 31 °C, animals demonstrated a clear avoidance of the 34 °C in the CPT, but failed to do so in the conventional TPP assay (**Figure S1**). This preference underscores the importance of integrating multiple sensory inputs — ambient "air" and contact temperatures — in forming a coherent thermal perception, a complexity often overlooked in simpler thermal assays.

Consistent with previous findings, our results reveal that the absence of TRPM2 impedes the development of a preference for warmer temperatures (8, 15). In contrast, animals lacking TRPV1 exhibited behavioural patterns similar to their wildtype counterparts, spending comparable amounts of total time in the warm chamber (**Figure 1E-F**).

Intriguingly, a finer characterization of the dynamics of the animal behaviour in the assay revealed differences between *Trpv1*$^{-/-}$ and *Trpm2*$^{-/-}$ animals, particularly in the frequency of crossings between chambers and the time spent in each chamber (**Figure 1G-H**). These behavioural nuances were further elucidated by modelling the behaviour with a drift-diffusion model (**Figure S5** and **Figure 5**). This model, a novel approach for such behavioural assays in general and for temperature as a sensory modality in particular, uncovered an impaired process of evidence accumulation within the warm chambers in *Trpm2*$^{-/-}$ animals. Moreover, we could explain the more frequent chamber crossings of *Trpv1*$^{-/-}$ animals by the fact that they accumulated evidence more erratically (**Figure 5I**).

Cellular insights into warm-temperature sensation

Cultures from *Trpv1*$^{-/-}$ animals exhibited a substantial decrease in the proportion of WSNs (**Figure 2**). This is similar to previous studies from trigeminal neurons, where the loss of TRPV1 led to a complete loss of warm-temperature responses (7). While the role of TRPV1 was more salient in the warm-temperature range, *Trpm2* knockouts displayed a reduction in temperature responsiveness across a broader spectrum, extending into hotter temperatures (**Figure 2**, **Figure S3**). This is in line with previous studies highlighting a loss in warmand heat-responsive cells in *Trpm2*$^{-/-}$ cells (8–10).

Interestingly, in initial experiments using DRG neurons from *Trpm2*$^{-/-}$ and *Trpv1*$^{-/-}$ animals cultured overnight, we were only able to show the necessity of TRPM2 for heat responses but failed to reproduce the previously reported reduction in WSNs in *Trpm2*$^{-/-}$ and *Trpv1*$^{-/-}$ sensory neurons (**Figure S3F**, (7, 8)). The inability to reproduce the aforementioned cellular phenotypes in cultured sensory neurons might be due to two factors: the abundance of WSNs and the variability in their proportions between experiments and animals (**Figure 2** and **Figure S3**). These require a larger sampling of sensory neurons from multiple animals for a reliable estimation of effects, something that is often lacking in previous studies of cellular warm-temperature-detection (8). Furthermore, overnight cultures, which are the *de facto* standard in the field, might be more akin to an injury model (**Figure S3**). The three-day cultures presented in this study allow the cells the time to partially regenerate from the harsh dissociation procedure (45), and pose an alternative that more closely resembles the physiological condition.

TRPV1: bridging cellular data with behavioural patterns

The cellular data predict that animals lacking TRPV1 would have large deficits in their ability to detect warm temperatures. Yet, overall, *Trpv1*$^{-/-}$ animals stay in the thermoneutral chamber for a similar proportion of time as wildtype controls. Analysis of the remaining WSNs in *Trpv1*$^{-/-}$ animals revealed a critical insight: these neurons predominantly respond during the static phase of the temperature stimuli.

In the CPT, animals frequently transition between chambers, experiencing rapid temperature changes upon crossing, but then spend most of their time in an isothermal environment (**Figure S1H**). This suggests that *Trpv1*$^{-/-}$ animals primarily rely on static temperature information for thermal detection, rather than rapidly fluctuating temperatures. This is reflected in the higher number of crossings between the different thermal chambers, coupled with shorter visits to the hotter chambers. This set of results led us to hypothesize that rapidly changing thermal information perceived during the transitions of the animals is not properly detected by *Trpv1*$^{-/-}$ animals. This hypothesis is further supported by the behavioural model (**Figure 5**). It indicates that, *Trpv1*$^{-/-}$ animals exhibit a higher drift rate in warmer test chambers, suggesting an avoidance of these temperatures. However, the increased noise in the driftdiffusion model points to a less reliable temperature detection mechanism. This implies that, despite the substantial loss of WSNs, the remaining neuronal population provides sufficient information for the detection of warmer temperatures, albeit with reduced precision.

The reduced precision might stem from the loss of dynamic temperature responders (**Figure 3**). These WSNs might be crucial in detecting a rapid change of temperature (e.g. when the animals move across different thermal environments). This is highlighted by findings from TRPV1-overexpressing animals. These animals, equipped with an enhanced ability to respond to dynamic temperature changes (**Figure 4**), have a higher drift rate and lower noise levels in warmer chambers in the model (**Figure 5**). These characteristics lead to a faster and more precise choice in the CPT. Combined, these results highlight the direct role of TRPV1, and its expression levels, in the precise temporal detection of warm temperatures.

TRPM2: cellular mechanisms and behavioural implications

A reversed scenario unfolds for TRPM2. The behavioural data suggests a strong deficit of sensory neurons to report warm temperatures. *Trpm2*$^{-/-}$ WSNs, while less abundant compared to WSNs from wildtype DRG cultures, do not exhibit marked differences in response dynamics. It is tempting to hypothesize, given the results from *Trpv1*$^{-/-}$-cultures, that TRPM2 affects the static phase of temperature detection. We conducted various analyses on the static responses of *Trpm2*$^{-/-}$ WSNs (data not shown), but failed to uncover significant differences to wildtype WSNs. This persistent discrepancy raises several hypotheses:

One explanation involves the specific population of WSNs reliant on TRPM2. Single-cell sequencing and functional analyses of dorsal root ganglia suggest that WSNs form two, genetically distinct populations, one of which prominently expresses *Trpm2* (46, 47). Different genetic/functional populations of sensory neurons often show diverging spinal innervation, with different upstream processing pathways (47–50). The genetic separation could hint at multiple neural innervation routes for innocuous temperature information. In this context, the loss of TRPM2 might specifically impair warm-temperature perception in thermoregulation-specific innervation pathways, without significantly affecting perceptual temperature discrimination performance (17).

The second explanation implies that the role of TRPM2 in temperature detection might extend beyond its expression in sensory neurons. Particularly, it is possible that TRPM2 mediates part of its effect via the hypothalamic preoptic area (POA), a temperature sensitive brain region involved in body temperature regulation (51). Preoptic TRPM2 has been shown to mediate autonomic thermoregulatory responses upon warmtemperature stimulation (52–54). Preoptic temperature pathways may not only drive autonomic thermoregulatory responses, but can also influence temperature preference behaviour (27, 51). Considering that, within the time frame of the chamber preference test, ambient temperature changes are directly transferred to the POA, it is possible – but not yet tested – that preoptic TRPM2 is involved in the choice of comfort-temperature.

Implications of findings

This study introduces an innovative behavioural assay, an improved protocol to culture DRG neurons, and methodologies for analysing animal behaviour in temperature preference assays. We emphasize the importance of examining the dynamics of perceptual decision-making and incorporating behavioural modelling. Significantly, we demonstrate that TRPV1 and TRPM2 channels contribute differently to temperature detection, supported by behavioural and cellular data. This research not only advances our understanding of thermal perception mechanisms but also adds new dimensions for integrating cellular and behavioural data to study the neural foundations of temperature sensation.

Acknowledgements

We thank Christina Steinmeier-Stannek, Annika von Seggern, Daniela Pimonov, Lisa Vierbaum, Amandine Cavaroc, and Lisa Weiler for technical support; members of the Siemens lab, particularly Hagen Wende, Katrin Schrenk-Siemens, and Jörg Pohle, for inspiring discussions and critical input. Additionally, the authors thank Juan Boffi, Katharine Shapcott, Natalie Schaworonkow, Marieke Schölvinck, and Martha Nari-Havenith for their support, discussions, scientific input and valuable criticism of the work. Funding: The authors gratefully acknowledge the data storage service SDS@hd supported by the Ministry of Science, Research and the Arts Baden-Württemberg (MWK) and the German Research Foundation (DFG) through grant INST 35/1314-1 FUGG. A.T. acknowledges support from the Margarita Salas Fellowship and the Joachim Herz Stiftung. This work was supported by the European Research Council ERC-CoG-772395 and the German research Foundation SFB/TRR 152 and SFB1158 (to J.S.).

Author contributions

M.A. and J.S. conceptualized the study. M.A. and G.K. designed, tested, and collected data with the CPT. M.A. analysed all the data from the CPT and modelling for the DDM. M.A. performed calcium imaging experiments, processed, and performed analysis for all cellular data. A.T. was involved in the analysis of the response characteristics of WSNs, as well as with model choices of the DDM. M.A. prepared the figures, with input from A.T. and J.S.. J.S. and G.K. acquired funding for the project. M.A. and J.S. wrote and edited the manuscript with input from G.K. and A.T..

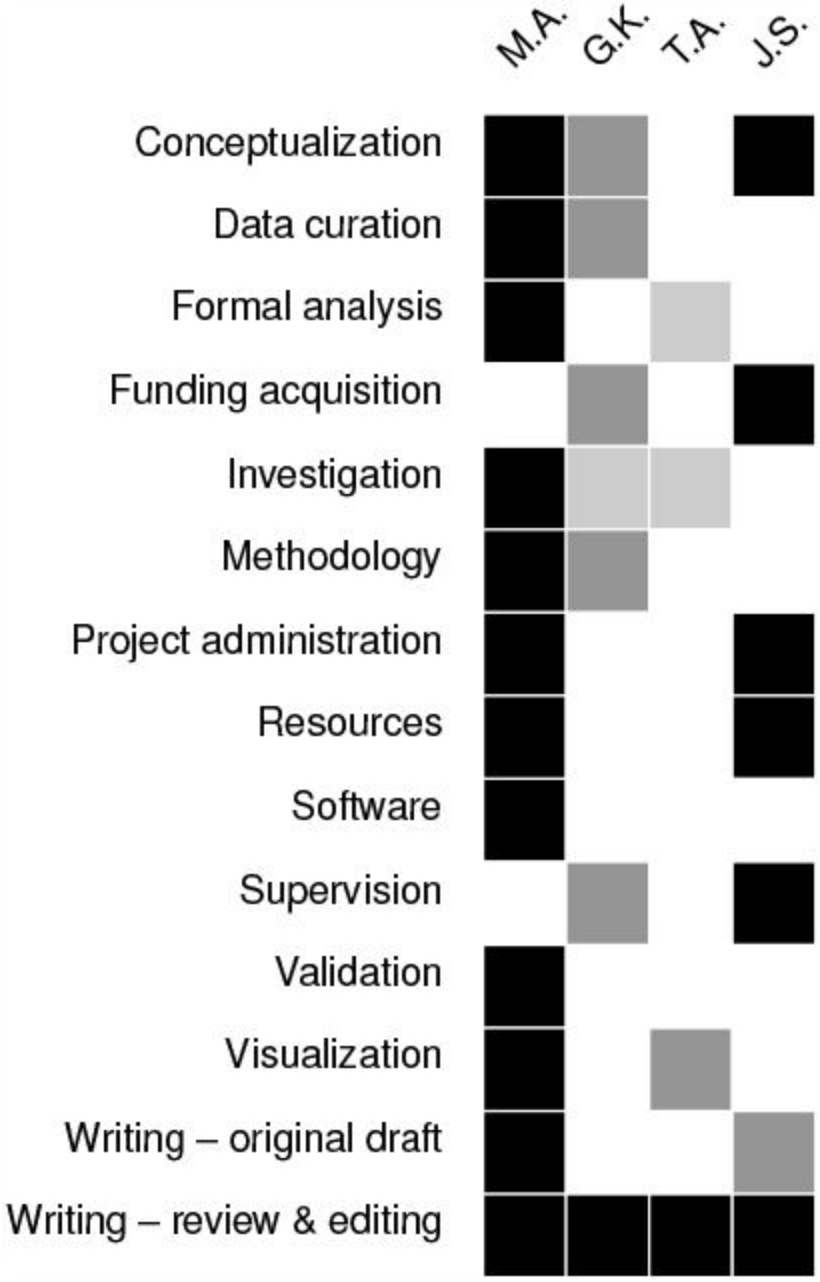

Supplementary Information

Key resource table

Resource Availability

Lead contact

Requests for resources and reagents should be directed to and will be fulfilled by the lead contact Jan Siemens (jan.siemens@pharma.uni-heidelberg.de).

Materials availability

This study did not generate any unique reagents.

Reagent	Source	Identifier
Experimental models: Organisms/strains		
Trpm2$^{-/-}$ mice: B6;Trpm2^{tm1Yamo}/Uhg	Yasuo Mori	MGI:3803341
Trpv1$^{-/-}$ mice: B6.129X1-^{Trpv1tm1Jul}/J	David Julius	MGI:1934023
Trpv1^{OX} mice: C57BL/6N-$^{Tg(Trpv1)5917Jsmn}$/J	Interfacultary Biomedical Faculty, University of Heidelberg	MGI:5629399
Wildtype mice: C57BL/6NRj	Janvier Laboratories	MGI:6236253
Trpv1^{cre} mice: B6.129-Trpv1$^{tm1(cre)Bbm}$/J	The Jackson Laboratory	RRID: IMSR_JAX:017769
Rosa-DTA mice : Gt(ROSA)26$^{Sortm1(DTA)Jpmb}$/J	The Jackson Laboratory	RRID: IMSR_JAX:006331
Trpv1^{Abl} mice: F1 of Trpv1^{cre} and RosaDTA	Interfacultary Biomedical Faculty, University of Heidelberg	
Trpm8$^{-/-}$ mice: Trpm8^{tm1Jul}	David Julius	MGI:3716518
Reagents and Liquids		
4-(2-hydroxyethyl)-1-piperazineethanesulfonic acid (HEPES)	Carl Roth	9105.4
Antibioic-Antimitotic (100X)	Thermo Fischer Scientific	15240062
Bovine serum albumin (BSA) fraction V	Carl Roth	T844.1
Cal-520 AM	AAT Bioquest	21130
Calcium chloride dihydrate	Merck Millipore	1023821000
Capsaicin	Tocris	462
Collagenase	Sigma	C0130
Dulbeccos' modified eagle media (DMEM)F12 without Glutamine	Thermo Fischer Scientific	21331046
Fetal calf serum (FCS) - EU Approved (South American)	Invitrogen	10270
Isoflurane	Baxter	HDG9623
L-alanyl-L-glutamine dipeptide (Glutamax Supplement 100X)	Invitrogen	35050
Laminin	Sigma	L2020
Magnesium chloride	Sigma Aldrich	M8266-1KG
Pluoronic F127 tenside	Invitrogen	P6866
Poly-D-Lysine (PDL)	Sigma	P7886
Potassium chloride	Labochem international	LC-5916.1
Proteinase K	Carl Roth	7528.1
Sodium chloride	Sigma Aldrich	31434-1KG-R
Tris-HCl	Carl Roth	5429.3
Trypsin-EDTA 0.05%	Thermo Fischer	25300054

Table S1.

List of organisms, reagents, software, and algorithms used in the study.

Dulbecco's PBS	Thermo Fischer Scientific	14040141
Software and algorithms		
LOGO! Soft Comfort	Siemens	
Metafluor	Molecular devices	
Miniscope DAQ acquisition software	UCLA Miniscope team	
Python 3.10	Python software foundation	
R 4.3.2	R core team	
ffmpeg 4.2		
Thermes USB Data Acquisition	Physitemp	
HSSM 0.1.5	https://github.com/lnccbrown/HSSM	
MINIROCKET as implemented in sktime	https://github.com/angus924/minirocket	
Suite2p	https://github.com/MouseLand/suite2p	
Cellpose	https://github.com/MouseLand/cellpose	

Table S1. (continued)

Data and code availability

Data

The datasets supporting the current study have not been deposited in a public repository, but are available from the corresponding author, Muad Abd El Hay, upon request.

Code

Analysis code to reproduce the finding and any additional information required to reanalyse the data reported in this paper is available from the corresponding author, Muad Abd El Hay, upon request.

Methods

Animals and housing

All animal care and experimental procedures were approved by the local council (Regierungspräsidium Karlsruhe, Germany) under protocol numbers G-201/16 and T05-19. Animals were kept under specific-pathogen-free (SPF) conditions and a 12-hour day-night cycle. Housing temperature and humidity were maintained at 22 ± 2 °C and 50 % to 60 %, respectively. Animals were fed ad-libitum with Altromin Rod 16 or Rod 18 animal food. The housing environment was enriched using Crincklets Nest-Pads and ABBEDD LT-E-001 bedding. For this study, only male animals were used, as we aimed to compare our results with previous studies which exclusively used male animals (7, 8, 17, 43). Mice between 6 and 25 weeks of age were used for the experiments.

Thermal preference chamber design, operation, and video capture

The thermal preference chamber consisted of two expanded polystyrene boxes connected using plastic glue and sealed with silicone (**Figure S1A**) with dimensions of 26.1 cm x 60.3 cm x 19.8 cm (w x l x h). The 4.3 cm-thick Styrofoam walls provided the necessary thermal insulation for the experiments. Inside the enclosure, the animals' movement was limited by a 13 cm x 31.4 cm x 15.5 cm steel cage placed on top of a stainlesssteel baseplate. To create two thermally isolated chambers, the enclosure, cage, and baseplate were adjusted to form a 4.3 cm x 6.3 cm x 6.3 cm tunnel. The baseplate and cage were custom-built by our institute's mechanical workshop. The cover combined foam and wood as insulators, with an acrylic glass inset for observation purposes.

Temperature within the chamber was regulated by two Peltier elements attached to heat sinks, each connected to a generic computer fan for efficient temperature distribution. To avoid overheating, the Peltier elements were connected to a Multitemp III circulating water pump (Amersham Biosciences) set to 28 °C. These elements were managed by a modified Siemens LOGO TD! controller, programmed for precise temperature adjustments, and accessed using the LOGO! Soft Comfort (Siemens) software. For monitoring, two Physitemp IT-18 flexible thermocouples were attached to the chamber walls, serving as reference thermometers. Data capture was conducted using a customer-grade webcam (Spedal), linked to the UCLA miniscope project's capture software, operating at 20 Hz to 30 Hz. The output files from each recording session were concatenated using *ffmpeg* software for subsequent processing. For control experiments using the two-plate temperature preference test (**Figure S1**, we used the BIO-T2CT system by BioSeb with the same camera setup as described above.

Thermal preference tests, processing, and analysis

Animals were transported to and acclimatized in the experimental room for at least 24 h before the experiments. The room maintained a dim light setting and a 12-hour day-night cycle. To ensure temperature stability, the setup was allowed to stabilize for 90 min before starting an experiment (**Figure S1B-D**). Once the setup reached a stable temperature, the lid was briefly opened (**Figure S1**), and an animal was placed into the enclosure, the lid closed again, and allowed to roam freely for at least 30 min, before replacing it with the next animal.

Due to the dim light conditions and the reflections on the cover of the enclosure (see **Figure 1** for an example), conventional animal tracking approaches that rely on image contrast failed to provide robust outputs (data not shown). Therefore, we employed a neural-network based approach, namely *DeepLabCut*, for tracking the animals in the setup (55). For this purpose, we trained a ResNet50 network to track specific points on the animal: the snout, right ear, left ear, body centre, tail base, and tail tip (**Figure 1**). Additionally, we tracked eight reference points (four cage corners and four cage tops) in the cage for normalization purposes. The same model was also trained on reference frames acquired using the BIO-T2CT system. The resulting model generalized well to both setups, ensuring comparability of the outputs.

The DeepLabCut predictions were then further curated by replacing bad predictions (< 95% likelihood) with missing values, and removing recording sessions where > 25% were missing (usually due to the animal escaping the inner cage). Furthermore, we removed sessions in which the animals showed excessive climbing behaviour (> 95% of time between upper and lower cage corners). For the remaining sessions, the missing values were linearly interpolated and the centroid of the ears, body centre, and tail-base was used as the position of the animals. The X- and Y-positions of the centroid were then scaled to the tracked cage corner points to correct for minor movements of the camera or the setup. The resulting X- and Y-position time courses were then downsampled to 1 Hz. Only the first 30 min of the recording were kept. Shorter sessions were removed.

Primary sensory neuron culture

Adult primary DRG cultures were prepared from 6-15 week old animals as described previously (37). Briefly, the animals were culled via isoflurane overdose, and their spinal columns excised and separated from muscle tissue. The spinal column was then cut lengthwise and the DRGs collected, freed from nerve branches, halved, and treated with a collagenase solution (1.25 mg/mL in Ringer's solution) for 1 h at 37 °C with gentle inversion every 15 min. This was followed by a 15 min trypsin digestion (2.5 mg/mL) at 37 °C, repeated trituration and suspension in complete culturing medium (DMEM/F12 w/o Glutamin,10% heat-inactivated FCS, 2 mM L-glutamine (Glutamax), 1x Anti-biotic/mitotic), and centrifugation at 900 rpm for 10 min over a BSA solution (150 mg/mL) to pellet the cells. The supernatant was discarded, the pellet was resuspended in culturing media, and spotted onto PDL- and Laminin-coated glass coverslips (5 mm). The cells were then left to settle onto the coverslip in the incubator for 1 h at 37 °C, and then covered with culturing media. Cultures were either used the following day (overnight) or kept for three days, with a medium change after the first day.

Calcium imaging recordings

For calcium imaging, cells cultured on coverslips were incubated for either one or three days. Before imaging, cells underwent a washing process with Ringer's solution (140 mM NaCl, 5 mM KCl, 2 mM $MgCl_2$, 2 mM $CaCl_2$, 10 mM glucose, and 10 mM HEPES, adjusted to pH 7.4.), followed by loading with the calcium-sensitive dye Cal520-AM (10 µM) and Pluronic acid F-127 (0.05 %) in Ringer's solution. The cells were incubated for 1 h at 37 °C, then the dye solution was replaced with Ringer's solution for a further 30 min at room temperature, minimizing light exposure.

The perfusion system, a ValveBank II (Automate) to control multiple inflows, and an air200 aquarium pump (Eheim) for outflow, was set to a maximum flow rate of 3 mL/min, facilitating laminar flow in the imaging chamber (RC-22, Warner Instruments). The coverslip was placed near the outlet to minimize movement artefacts. An IT-18 thermocouple (physitemp) was placed close to the coverslip to record the chamber temperature. Imaging settings varied based on the camera used: for CoolSnapHQ2 (Photometrics), exposure was set at 5 ms with 3x gain and 3×3 binning, whereas for Zyla 4.2 (Andor Technology), it was 80 ms with 2×2 binning. We used a Lambda DG-4 as a light source, maintained at 30 % intensity to reduce bleaching.

Images were captured using *MetaFluor* software at 4 Hz or 10 Hz frequencies. Standard experiments involved a 1 min baseline, 25 s stimuli, followed by a 3 min to 5 min recovery period with room-temperature Ringer's solution (Figures **Figure 2** and **Figure S3**). To identify TRPV1-positive neurons, we used the agonist Capsaicin (1 µM, (3)). A Ringer's solution with a high potassium concentration (100 mM KCl) was used as a final stimulus to identify neurons. Solutions were heated via glass coils connected to a heated water bath. Each FOV was imaged for a maximum of 60 min, and the usage of coverslips was limited to 2 h post-loading with the dye.

Calcium imaging preprocessing and analysis

Calcium imaging data were motion-corrected and pre-processed using *Suite2p* (56). Cell regions of interest (ROIs) were identified using the *Cellpose* package integrated into *Suite2p* (57). The mean fluorescence of cells and surrounding neuropil was calculated by *Suite2p*, and neuropil contamination was corrected by subtracting 70 % of the background neuropil traces from each cell's fluorescence trace. The corrected data was then imported into a custom R-package, *neuroimgr*, for further analysis in R (*https://github.com/hummuscience/neuroimgr*).

Normalization was performed using the $\Delta F/F_0$ method, where baseline fluorescence (F_0) is calculated as the mean fluorescence of the baseline, and ΔF is the change in fluorescence over time. For heatmaps, F_0 was estimated using the first 10 s of the experiments. For individual stimuli, the mean of the first 10 frames was used as F_0. Heatmaps were generated using the *ComplexHeatmap* R package. Cells were sorted by the earliest time point where they cross 10 % of their cumulative $\Delta F/F_0$ in a given FOV and clustered using the Ward D2 algorithm. $\Delta F/F_0$ values smaller than the 0.1 and larger than the 99.9 percentile were clipped.

Due to the temperature-sensitivity and loading variability of the calcium dye, a threshold-based approach failed to reliably identify responding cells across experimental days and FOVs (58). Therefore, we used time series classification to identify temperature-responsive cells. For this, calcium traces for each cell and stimulus were normalized, downsampled to 4 Hz, and a sample of 1000 traces across stimuli was manually labelled to create a training dataset. This ground-truth dataset was used to evaluate multiple time series classification algorithms, with MINIROCKET (as implemented in the *sktime* Python package, (59)) yielding the best results (data not shown). The trained classifier was then applied to the remaining cells to identify temperature-responsive cells. A similar approach was used to identify capsaicin-responsive cells. Cells that did not respond to any of the applied stimuli were excluded from the analysis.

Drift-diffusion model

We employed a Drift-Diffusion Model (DDM) to analyse the behaviour of mice in thermal chamber experiments. The DDM was preferred over simpler models like the Markov switching model, as the latter did not provide satisfactory fits to our data (data not shown). Each parameter in the model can either be fit as a predictor (dependent on genotype, temperature combination, and temperature), fit to the entire data (floating), or fixed to a certain value. A typical drift diffusion model as described in (44) can drift to the upper or lower bound (representing two choices), but our experimental design only offers one choice (to leave the chamber). To reduce the probability of reaching the lower bound, and thereby improve the fit, we fixed the starting point/bias (z) to

0.9. This ensures that the evidence accumulation starts at a point that is much closer to the upper bound (a) than to the lower bound ($-a$). To choose the best combination of parameters that fits the data, we fit all the data to all remaining combinations of v, sv, and a (**Figure S5A** and **B**) and compared them via the expected log pointwise predictive density (ELPD) by Pareto smoothed importance sampling leave-one-out cross-validation (LOO) (60). Unreliable models as per (60) were discarded. The chosen model was constructed to account for variations in both noise (sv) and drift rate (v) for each genotype, temperature comparison, and chamber/temperature (**Figure S5A** and **B**, and **Equation 1**). To accommodate individual differences among animals, we introduced a random effect for each animal in the model. This approach enabled us to capture the unique behavioural patterns of each subject while assessing the general trends across the population.

$$v \mid sv \sim \text{temperature combination} \times \text{chamber} \times \text{genotype} + (1 \mid \text{animal}) \quad (1)$$

To fit the model, we applied a hierarchical Markov Chain Monte Carlo (MCMC) sampling approach as implemented in the *HSSM* python package. For the implementation of the hierarchical MCMC, we utilized the No-U-Turn Sampler (NUTS) as implemented in *NumPyro*, a robust algorithm for efficiently sampling from high-dimensional probability distributions. The tuning phase for all fit models involved 2000 samples, ensuring adequate exploration of the parameter space and helping to achieve convergence. The final model was run with four chains, each drawing 2000 samples.

Statistical methods

Statistical analyses were conducted using R software. Two-sample T-tests with False-discovery rate correction (FDR) were utilized for hypothesis testing involving two groups, and Wilcoxon tests with FDR correction were applied for non-parametric data, facilitated by the *rstatix* package. To assess differences in crossing behaviour, a Cox proportional hazard model was used, as implemented in the *survival* package. For visit length comparisons, a mixed-effects model was fit using the *lme4* package, allowing random effects for animal subjects where appropriate. Multiple comparisons for the mixed-effects and Cox models were accounted for using the FDR approach within the *emmeans* and *multcomp* packages. All statistical tests are summarized in S2. Only statistically significant results ($p < 0.05$) are shown, except in cases where none of the tested contrasts were significantly different.

Supplementary tables and figures

Figure	Sample sizes	Statistical test	Results
1F	34 °C: Wildtype (41), *Trpv1*$^{-/-}$ (12), *Trpm2*$^{-/-}$ (20)	t-test with FDR for multiple corrections	6 min: *Trpm2*$^{-/-}$ vs Wildtype, p = 0.035, ; *Trpv1*$^{-/-}$ vs Wildtype, p = 0.005,
			15 min: *Trpm2*$^{-/-}$ vs Wildtype,p = 0.015,
			18 min: *Trpm2*$^{-/-}$ vs Wildtype,p = 0.025,
			27 min: *Trpm2*$^{-/-}$ vs Wildtype,p = 0.044,
	38 °C: Wildtype (42), *Trpv1*$^{-/-}$ (15), *Trpm2*$^{-/-}$ (23)		18 min: *Trpm2*$^{-/-}$ vs Wildtype, p = 0.012,
			21 min: *Trpm2*$^{-/-}$ vs Wildtype, p = 0.033,
			27 min: *Trpm2*$^{-/-}$ vs Wildtype, p = 0.024,
			30 min: *Trpm2*$^{-/-}$ vs Wildtype, p = 0.011,
1H	34 °C: Wildtype (41), *Trpv1*$^{-/-}$ (12), *Trpm2*$^{-/-}$ (20)	Cox model of crossing times + FDR	*Trpv1*$^{-/-}$ vs. Wildtype: Estimate 0.246, p = 7.07e-05
	38 °C: Wildtype (42), *Trpv1*$^{-/-}$ (15), *Trpm2*$^{-/-}$ (23)		*Trpm2*$^{-/-}$ vs. Wildtype: Estimate -0.310, p = 1.44e-06
			Trpm2$^{-/-}$ vs. Wildtype: Estimate 0.017, p = 0.759, ns
			Trpv1$^{-/-}$ vs. Wildtype: Estimate 0.393, p = 3.13e-12
	34 °C: Wildtype (41), *Trpv1*$^{-/-}$ (12), *Trpm2*$^{-/-}$ (20)	Mixed-effects model + FDR	*Trpm2*$^{-/-}$ vs. Wildtype: Estimate 31.349, p = 1.27e-06
	38 °C: Wildtype (42), *Trpv1*$^{-/-}$ (15), *Trpm2*$^{-/-}$ (23)		*Trpm2*$^{-/-}$ vs. Wildtype: Estimate 13.035, p = 0.00936
2D	Wildtype (18), *Trpv1*$^{-/-}$ (10), *Trpm2*$^{-/-}$ (12) FOVs	t-test with FDR correction	First: *Trpv1*$^{-/-}$ vs. Wildtype, p= 0.000814,
			Second: *Trpv1*$^{-/-}$ vs. Wildtype, p = 0.005 ; *Trpm2*$^{-/-}$ vs. Wildtype, p = 0.049
			Third: *Trpv1*$^{-/-}$ vs. Wildtype, p = 0.026 ; *Trpm2*$^{-/-}$ vs. Wildtype, p = 0.026
3E	First Stimulus: Wildtype (95), *Trpv1*$^{-/-}$ (14), *Trpm2*$^{-/-}$ (47)	Wilcoxon test with FDR correction	*Trpv1*$^{-/-}$ vs. Wildtype: p = 0.033
	Second Stimulus: Wildtype (120), *Trpv1*$^{-/-}$ (25), *Trpm2*$^{-/-}$ (60)		*Trpv1*$^{-/-}$ vs. Wildtype: p = 0.011
	Third Stimulus: Wildtype (389), *Trpv1*$^{-/-}$ (99), *Trpm2*$^{-/-}$ (197)		*Trpv1*$^{-/-}$ vs. Wildtype: p = 0.0000676
4E	Second: Wildtype (245), *Trpv1*^{OX} (660)	Wilcoxon test with FDR correction	*Trpv1*^{OX} vs. Wildtype: p = 0.00034
4G	34 °C: Wildtype (41), *Trpv1*^{OX} (12)	t-test with FDR correction	9 min: *Trpv1*^{OX} vs. Wildtype, p = 0.002
			12 min: *Trpv1*^{OX} vs. Wildtype, p = 0.000849
			21 min: *Trpv1*^{OX} vs. Wildtype, p = 0.0128
			24 min: *Trpv1*^{OX} vs. Wildtype, p = 0.00437
	38 °C: Wildtype (42), *Trpv1*^{OX} (12)		3 min: *Trpv1*^{OX} vs. Wildtype, p = 0.0143
			15 min: *Trpv1*^{OX} vs. Wildtype p = 0.01
			21 min: *Trpv1*^{OX} vs. Wildtype p = 0.0476
4H	34 °C: Wildtype (41), *Trpv1*^{OX} (12)	Cox model + FDR	*Trpv1*^{OX} vs. Wildtype, Estimate: -0.309, p = 0.0000508
			Trpv1^{OX} vs. Wildtype, Estimate: -0.145, p = 0.0451
	38 °C: Wildtype (42), *Trpv1*^{OX} (12)	Mixed-effect model of visit lengths + FDR	[No Significant Results]
S1 I	25 °C: Wildtype (CPT: 11, TPT: 11), *Trpm2*$^{-/-}$ (CPT: 16, TPT: 17)	t-test with FDR correction	*Trpm2*$^{-/-}$ CPT vs. TPT, p = 0.00318
	34 °C: Wildtype (CPT: 12, TPT: 12), *Trpm2*$^{-/-}$ (CPT: 17, TPT: 17)		Wildtype CPT vs. TPT, p = 0.00137
	38 °C: Wildtype (CPT: 12, TPT: 12), *Trpm2*$^{-/-}$ (CPT: 17, TPT: 17)		*Trpm2*$^{-/-}$ CPT vs. TPT: p = 0.00312
S1 K	34 °C: Wildtype (41), *Trpv1*^{Abl} (13)	t-test with FDR correction	6 min: *Trpv1*^{Abl} vs. Wildtype, p = 0.00769
			12 min: *Trpv1*^{Abl} vs. Wildtype, p = 0.0287

Table S2.

Samples sizes and summary statistics. Only significant results (p < 0.05) shown. The exceptions are cases in which no statistically significant result was obtained in all comparisons of a test.

			15 min: *Trpv1*^{Abl} vs. Wildtype, p = 0.000436
			18 min: *Trpv1*^{Abl} vs. Wildtype, p = 0.000848
			24 min: *Trpv1*^{Abl} vs. Wildtype, p = 0.0166
			27 min: *Trpv1*^{Abl} vs. Wildtype, p = 0.0222
			30 min: *Trpv1*^{Abl} vs. Wildtype p = 0.0333
S2 B	25 °C: Wildtype (21), *Trpv1*$^{-/-}$ (11), *Trpm2*$^{-/-}$ (15)	t-test with FDR correction	[No Significant Results]
S2 C	25 °C: Wildtype (21), *Trpv1*$^{-/-}$ (11), *Trpm2*$^{-/-}$ (15)	Cox model of crossing times + FDR	*Trpm2*$^{-/-}$ vs. Wildtype Estimate: -0.478, p = 0.00000000194
		Mixed-effect model of visit lengths + FDR	[No Significant Results]
S2 F	34 °C: Wildtype (41), *Trpm8*$^{-/-}$ (12)	t-test with FDR correction	3 min: *Trpm8*$^{-/-}$ vs. Wildtype, p = 0.0056
			27 min: *Trpm8*$^{-/-}$ vs. Wildtype, p = 0.0268
	38 °C: Wildtype (42), *Trpm8*$^{-/-}$ (12)		12 min: *Trpm8*$^{-/-}$ vs. Wildtype, p = 0.0212
			27 min: *Trpm8*$^{-/-}$ vs. Wildtype, p = 0.000106
S2 G	25 °C: Wildtype (21), *Trpm8*$^{-/-}$ (8)	Cox model of crossing times	*Trpm8*$^{-/-}$ vs. Wildtype, Estimate: -0.408, p = 0.00000394
	25 °C: Wildtype (21), *Trpm8*$^{-/-}$ (8)	Mixed-effect model of visit lengths	*Trpm8*$^{-/-}$ vs. Wildtype, Estimate: 10.3, p = 0.0436
	34 °C: Wildtype (29), *Trpm8*$^{-/-}$ (8)	Cox and mixed-effects models	[No Significant Results]
	38 °C: Wildtype (28), *Trpm8*$^{-/-}$ (8)	Mixed-effect model of visit lengths	[No Significant Results]
S3 C	First: Overnight (8), Threeday (43)	t-test with FDR correction	p = 0.0297
	Second: Overnight (8), Threeday (43)		p = 0.00247
	Third: Overnight (8), Threeday (43)		p = 0.00247
	Fourth: Overnight (8), Threeday (35)		p = 0.0441
S3 F	First: Wildtype (8), *Trpv1*$^{-/-}$ (6), *Trpm2*$^{-/-}$ (6)	t-test with FDR correction	P = 0.02
	Second: Wildtype (8), *Trpv1*$^{-/-}$ (6), *Trpm2*$^{-/-}$ (6)		P = 0.02
S3 J	Wildtype (18) vs. *Trpv1*$^{-/-}$ (10) and *Trpm2*$^{-/-}$ (12)	t-test with FDR correction	Fourth: *Trpm2*$^{-/-}$ vs. Wildtype, p = 0.000124
			Fifth: *Trpm2*$^{-/-}$ vs. Wildtype, p = 0.01
S4 C	First: Wildtype (95), *Trpv1*$^{-/-}$ (14), *Trpm2*$^{-/-}$ (47)	Wilcoxon test with FDR correction	p = 0.033
	Second: Wildtype (120), *Trpv1*$^{-/-}$ (25), *Trpm2*$^{-/-}$ (60)		p = 0.011
	Third: Wildtype (389), *Trpv1*$^{-/-}$ (99), *Trpm2*$^{-/-}$ (197)		p = 0.0000676
	Fourth: Wildtype (1376), *Trpv1*$^{-/-}$ (663), *Trpm2*$^{-/-}$ (1032)		P = 0.000378
S4 F	First: *Trpv1*$^{-}$ (71), *Trpv1*$^{+}$ (113)	Wilcoxon test with FDR correction	P = 0.00000526
	Second: *Trpv1*$^{-}$ (141), *Trpv1*$^{+}$ (360)		P = 0.00000064
	Third: *Trpv1*$^{-}$ (182), *Trpv1*$^{+}$ (600)		P = 0.000000000511
	Fourth: *Trpv1*$^{-}$ (279), *Trpv1*$^{+}$ (517)		P = 0.00497

Table S2. (continued)

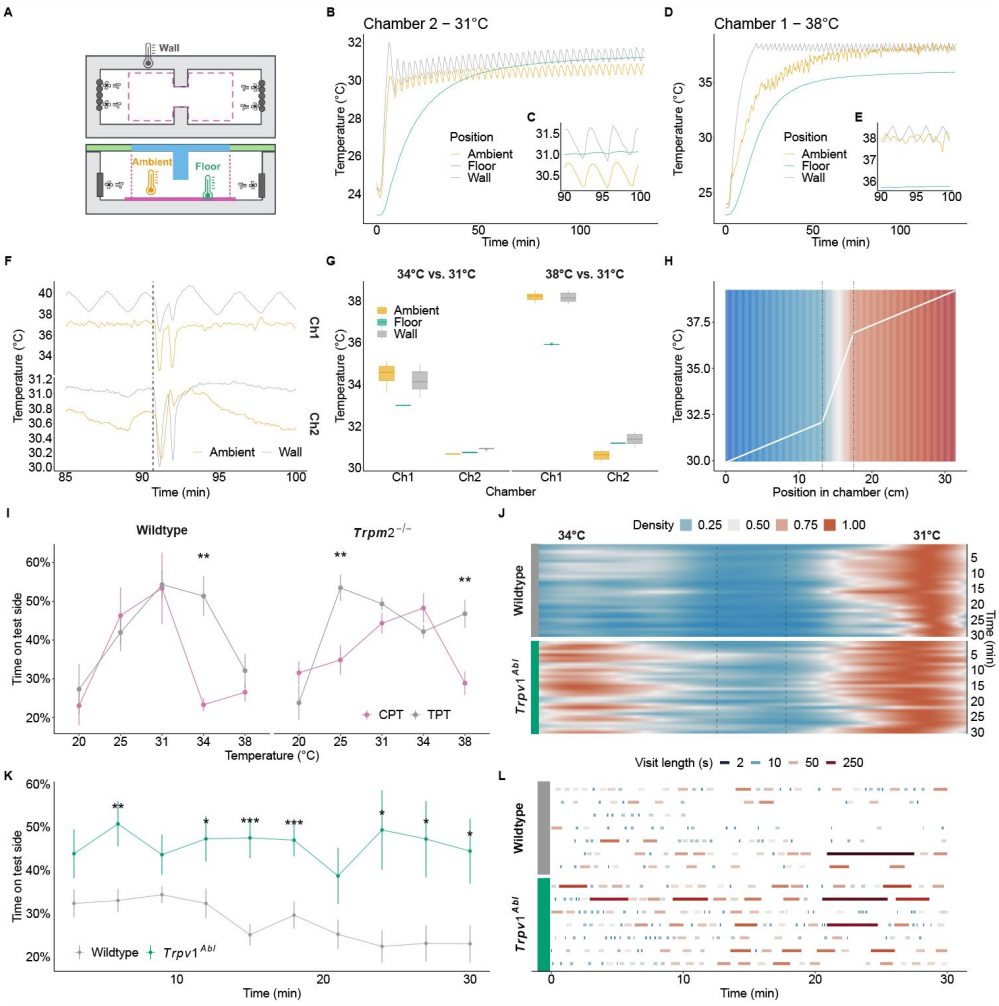

Fig. S1.

Establishing a novel ambient temperature preference test. Related to Figure 1.

A Schematic of the chamber preference test (CPT) from the top (upper panel) and side (lower panel). A styrofoam enclosure ensures adequate thermal isolation (grey shading). Peltier elements (dark grey ovals) equipped with fans allow the rapid circulation of heat throughout the chamber. Two wall thermometers allow monitoring and regulation of the chamber temperature in a closed-loop fashion. A steel cage (dashed pink line) marks the area where the animals move around freely. A stainless-steel floor (pink) allows easy clean-up and adaptation of the ambient temperature. A transparent top (blue) allows video recording and tracking of the animal position throughout the experiment. Two ambient and floor thermometers were used to calibrate the corresponding wall thermometer to achieve the desired ambient temperature in each chamber. **B** and **D** Exemplary temperature development at the beginning of an experimental day for each chamber and thermometer indicated in **A**. Neutral chamber set to 31 °C shown in **D**. Test chamber set to 38 °C shown in **B**. Insets **C** and **E** zoom-in onto the temperature recordings once the chambers stabilized (around 90 minutes of pre-warming). **F** Stability of ambient and wall temperature in chamber 1 (Ch1) and 2 (Ch2) when opening the enclosure to replace animals. The dashed line shows the time point of opening the enclosure. Floor temperature remained unaffected (data not shown). **G** Shown are wall, ambient, and floor temperatures at 31 °C neutral temperature and 34 °C or 38 °C test temperatures in chamber 1 (Ch1) and chamber 2 (Ch2). **H** Calculated ambient temperature gradient in the CPT at 31 °C neutral and 38 °C test temperatures. The dashed line shows the tunnel connecting both chambers. **I** Comparison of CPT and conventional TPT temperature preference assays in the same cohort of wildtype (n = 12) and *Trpm2*$^{-/-}$ (n = 17) animals, shown in CPT (**Figure 1**). **J** Density maps of the x-position of wildtype (n = 41) and thermally ablated animals (*Trpv1*^{Abl}, n = 13) at 31 °C vs 34 °C. Binned in 1-minute bins, concatenated, and interpolated. Dashed lines represent the tunnel connecting both chambers. **K** Proportion of time spent on the test side of animals shown in **J. L** Overview of the frequency and length of the visits to the test chamber 7 randomly sampled animals from **J** and **K**. Each visit is coloured by the log2 of its length to highlight varying visit lengths. * (p <0.05), ** (p <0.01), *** (p <0.001). See Table S2 for statistical details.

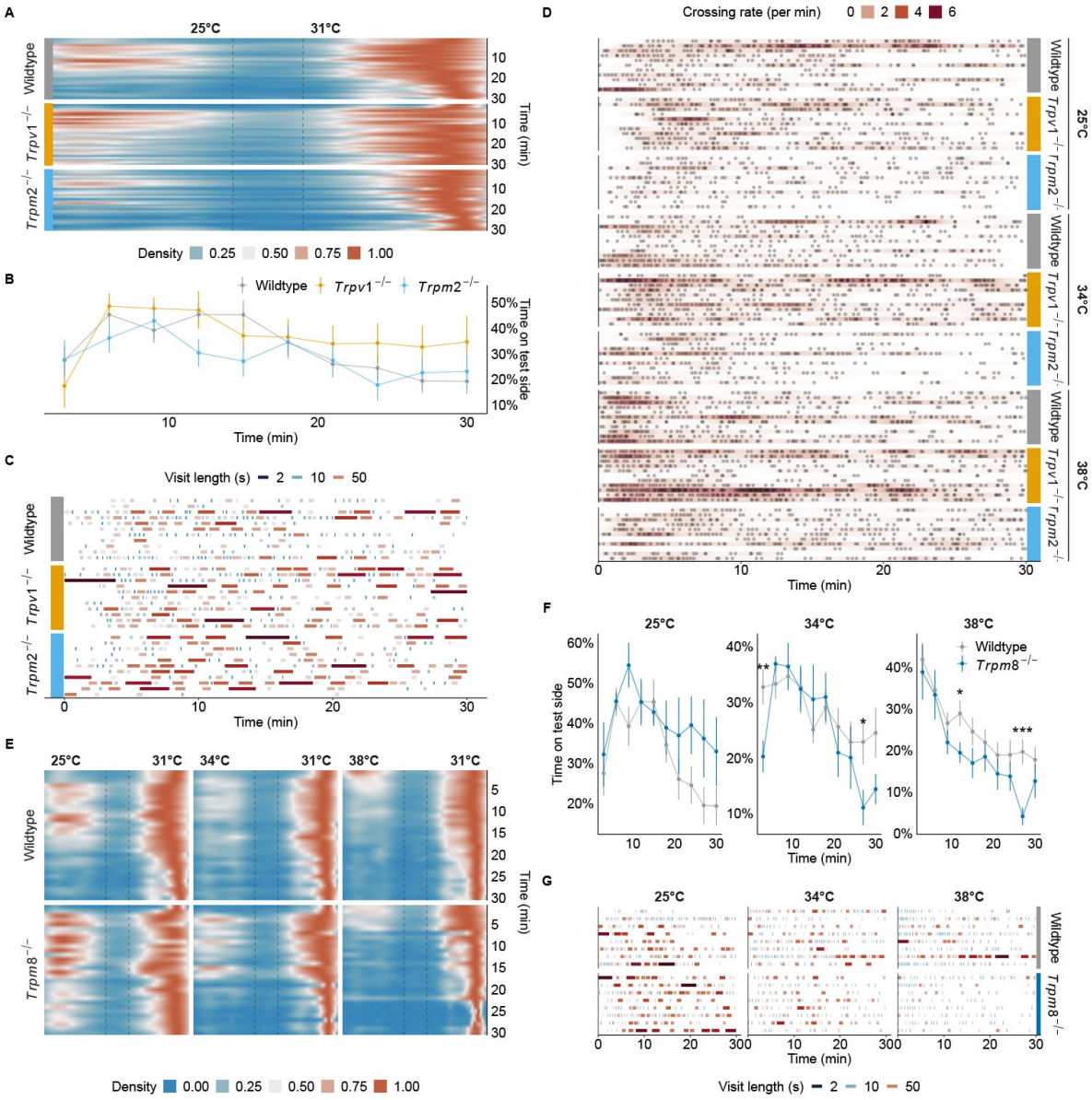

Fig. S2.

Temperature preference behaviour of all genotypes to 25 °C including *Trpm8*$^{-/-}$ animals.

Related to Figure 1. **A** Density maps of the x-position of the animals shown in CPT (**Figure 1**) when given the choice of 25 °C and 31 °C (reference temperature), over time. **B** Proportion of time spent at 25 °C for animals from **A. C** Visit lengths to the 25 °C chamber over time for 11 randomly sampled animals per genotype from **A. D** Crossing behaviour of animals from CPT (**Figure 1**) at different testing temperatures, over time. Each row represents one of 11 randomly sampled animals from each genotype at the indicated temperatures. Each dot is a crossing event from one chamber to the other. The colour denotes the variability in crossing rate (crosses per minute) for each animal. **E** Density occupation map of the *Trpm8*$^{-/-}$ animals at different test temperatures, over time. **F** Proportion of time spent at test side in 3-minute bins of animals from **E**. Visit lengths to the 25 °C chamber over time for animals in **E. G** Overview of the frequency and length of the visits to the test chamber for 8 randomly sampled animals per genotype and temperatures from **E**. Each visit is coloured by the log2 of its length to highlight varying visit lengths. * (p <0.05), *** (p <0.001). See Table S2 for statistical details.

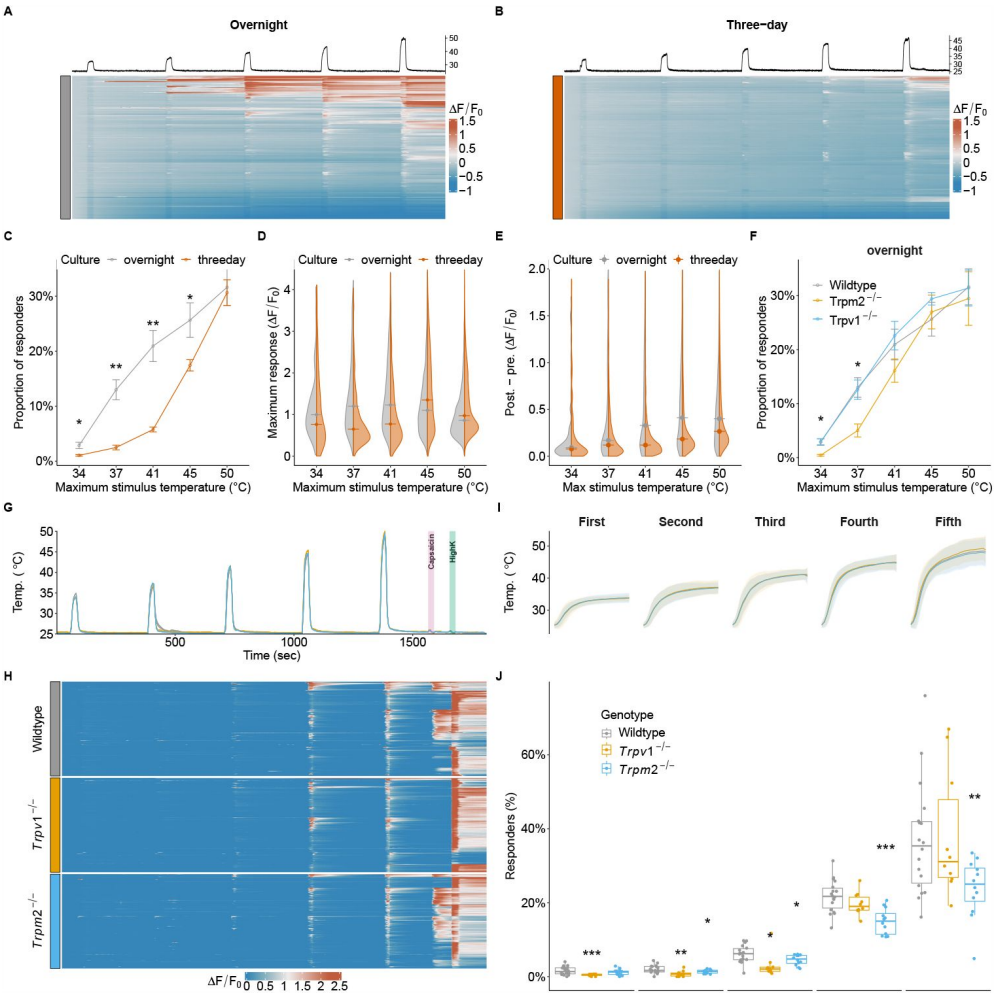

Fig. S3.

Comparison of culturing conditions for primary sensory neurons and their response to warm and hot temperatures.

Related to Figure 2. **A** and **B** Heat map showing normalized calcium responses ($\Delta F/F_0$) of individual cells (each row represents 1 cell) of a single FOV of 300 randomly sampled primary DRG neurons cultured overnight (**A**) or for three days (**B**) in response to 5 consecutive and increasing temperature stimuli. **C** Fraction of responding cells in relation to all imaged cells for overnight and three-day cultures in response to the temperature stimuli. Means and SEMs of overnight (4 animals, 8 FOVs, 2028 cells) and three-day (15 animals, 43 FOVs, 21149 cells) cultures. **D** Split violin plots showing the distributions of the maximum $\Delta F/F_0$ for all responding cells during each stimulus. **E** The post- and pre-stimulus difference for each cell in each stimulus for both conditions. A window of 25 seconds before and after each stimulus was used to calculate the mean $\Delta F/F_0$ for each window. A difference of 0 indicates that a cell was able to completely return to its baseline after responding to the stimulus. **F** The proportions of responders to each temperature stimulus in relation to all imaged neurons in cells cultured overnight from wildtype (4 animals, 8 FOVs, 2028 cells), *Trpv1*$^{-/-}$ (2 animals, 6 FOVs, 1714 cells), and *Trpm2*$^{-/-}$ (3 animals, 5 FOVs, 1816 cells). **G and H** Experimental paradigm of temperature stimulation. Five sequential and increasing temperature stimuli of 25 seconds with 5 minutes inter-stimulus intervals followed by capsaicin (1μM) and high potassium stimulation. Capsaicin was used to identify TRPV1-positive cells and high potassium to identify neuronal cells. The traces represent mean temperatures of the FOV shown in **H. H** Examples of normalized ($\Delta F/F_0$) calcium responses of temperature-sensitive cells sampled from all FOVs and experiments (n = 250 cells per genotype). **I** Mean and standard deviation of the five temperature stimuli applied. **J** The proportions of responders to each temperature stimulus in relation to all imaged neurons from wildtype (7 animals, 21 FOVs, 6928 cells), *Trpv1*$^{-/-}$ (5 animals, 17 FOVs, 5410 cells), and *Trpm2*$^{-/-}$ (6 animals, 18 FOVs, 6131 cells). Each dot represents an individual FOV. Note that the fraction of WSNs is small (6 ± 3 %) and therefore necessitates large sample sizes for robust estimations of effects caused by gain- and loss-of-function models. * (p <0.05), ** (p <0.01), *** (p <0.001). See Table S2 for statistical details.

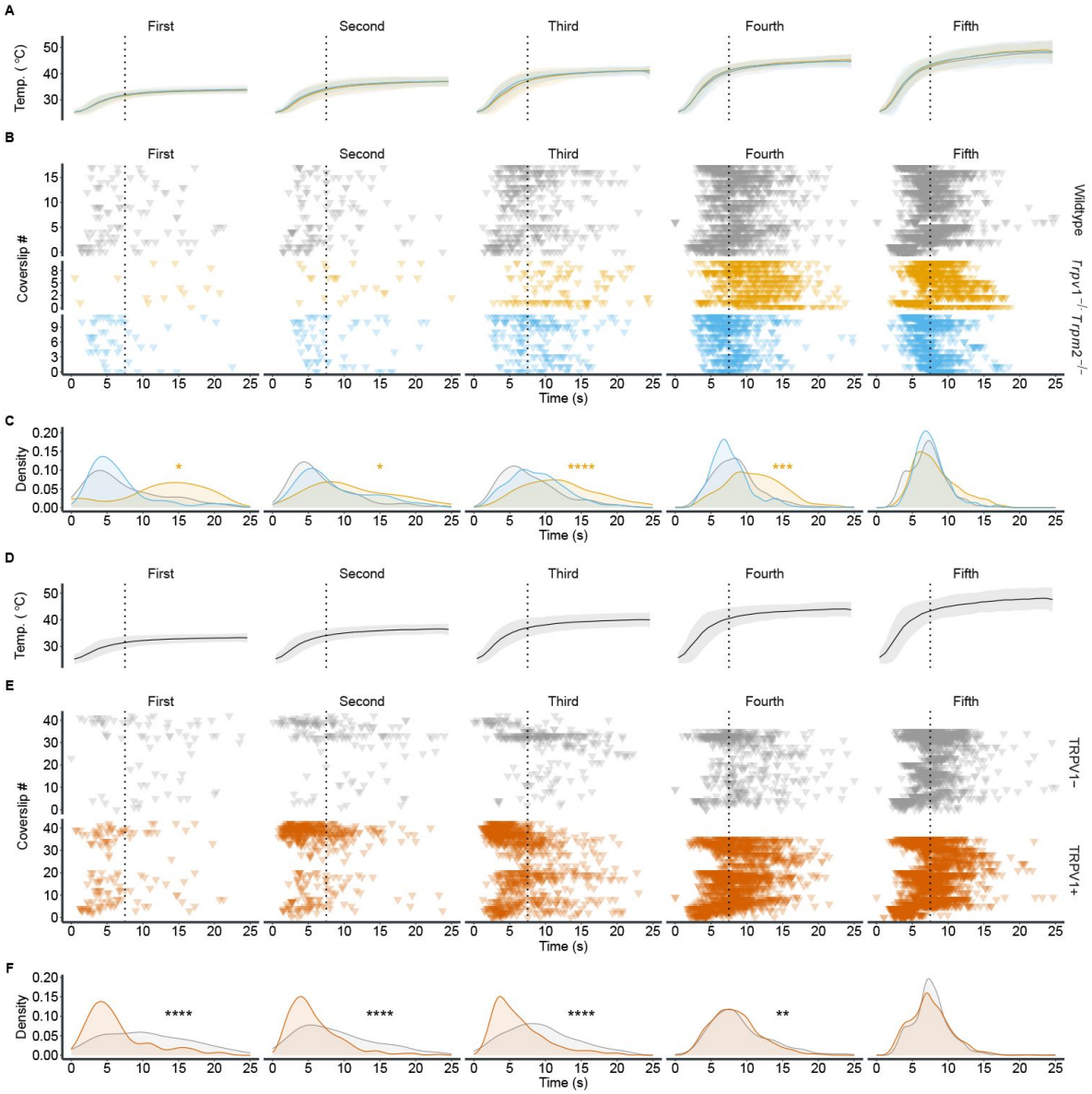

Fig. S4.

Responses to dynamic and static segments of warm and hot temperature stimuli.

Related to Figures 3 and 4. A Mean and standard deviation of the five warm-temperature stimuli applied. The dotted line indicates the transition between the dynamic and the static phases of the temperature stimuli. **B** Response initiation of all temperature-responsive cells imaged. Each row represents a FOV. Each triangle denotes the time point at which the cell begins to respond to the stimulus. Dotted line as in **A. C** Density representations of response time points for each genotype and stimulus. **D** and **E** same as **A** and **B**, except that only wildtype DRG cultures are included; cells are separated into two subgroups based on their responsiveness to capsaicin (orange: responsive, grey: non-responsive). **F** Density estimates of the response time points shown in **E**. * ($p < 0.05$), *** ($p < 0.001$), **** ($p < 0.0001$). See Table S2 for statistical details.

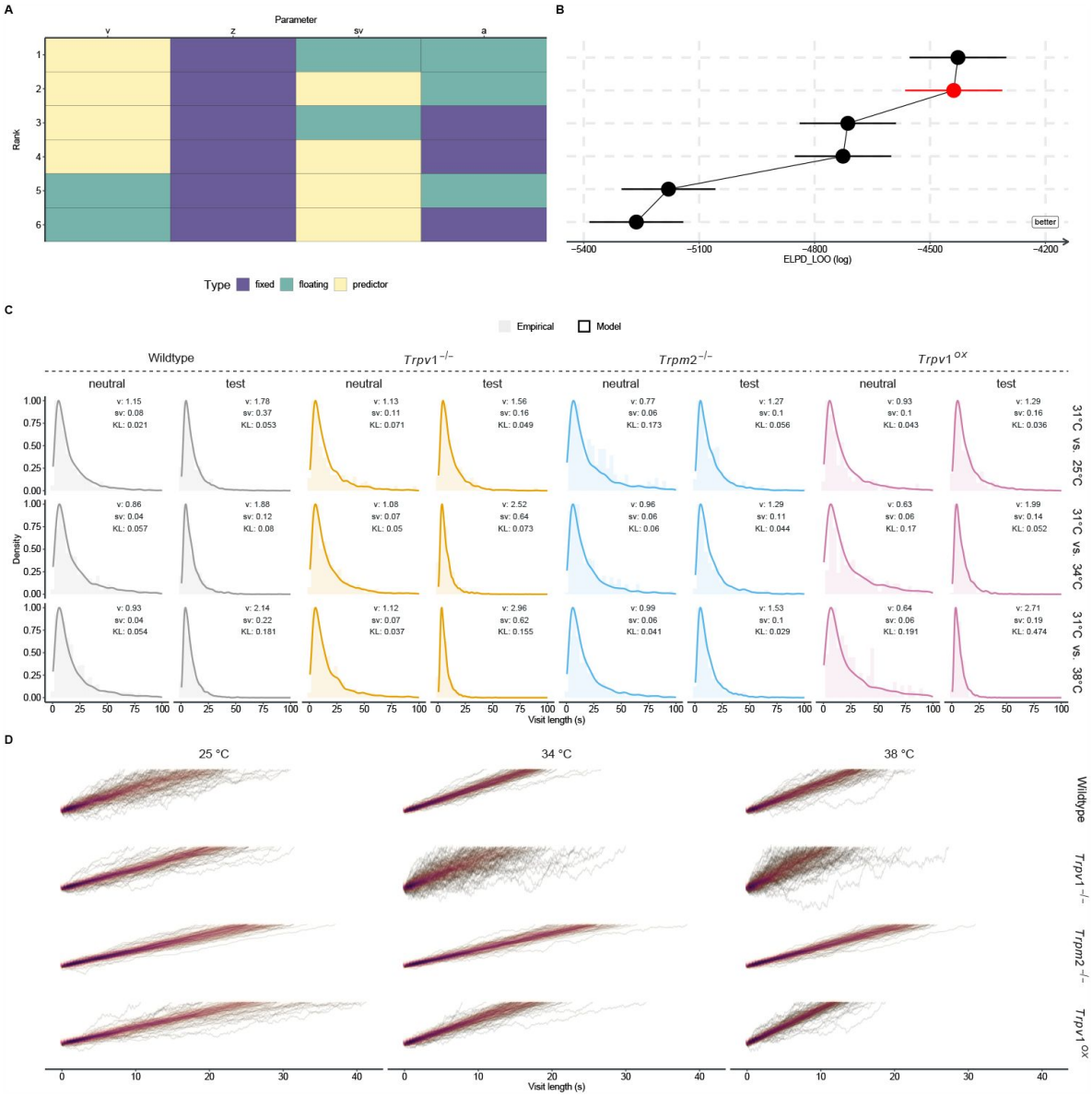

Fig. S5.

Model fits and DDM simulations for all genotypes and test temperatures.

A and B Comparison of different model parameter combinations. To ensure that the DDM only reaches the upper bound, the bias *z* was kept fixed to 0.9, while all other parameters were allowed to either be predictors or fit to the entire data (floating) (**A**). Model performance was compared and ranked by calculating the expected log pointwise predictive density (ELPD) by Pareto smoothed importance sampling leave-one-out cross-validation (LOO) (**B**). Horizontal error bars depict the standard error of the ELPD-LOO. The chosen model is indicated in red. **C** Density estimates and histograms for collected empirical data (histogram) and 1000 simulated trials (density – solid line) using the medians for drift and noise estimated for each genotype and chamber via Markov chain Monte Carlo (MCMC). Insets detail the temperature of the chamber, the used values for drift (*v*) and noise (*sv*), and the Kullback-Leibler divergence (KL) between the simulated distribution and the empirical data. **D** Simulated evidence accumulation processes for each genotype and test temperature for a 30-minute experiment. Parameters for drift, noise, and bound (starting point fixed to 0.88) were sampled randomly from the MCMC chains. Each line represents a trial. The plots are overlaid with a two-dimensional density of the resulting points, to highlight the general trajectory and the spread of the process.

References

1. Zotterman Yngve (1936) **Specific action potentials in the lingual nerve of cat** *Skandinavisches Archiv Für Physiologie* **75**:105–119 https://doi.org/10.1111/j.1748-1716.1936.tb01558.x

2. Hensel H., Schafer K., Ring E. Francis J., Phillips Barbara (1984) **Thermoreception and Temperature Regulation in Man** *Recent Advances in Medical Thermology* :51–64 https://doi.org/10.1007/978-1-4684-7697-2_8

3. Caterina Michael J., Schumacher Mark A., Tominaga Makoto, Rosen Tobias A., Levine Jon D., Julius David (1997) **The capsaicin receptor: A heat-activated ion channel in the pain pathway** *Nature* **389**:816–824

4. Peier A.M., Moqrich A., Hergarden A.C., Reeve A.J., Andersson D.A., Story G.M., Earley Dragoni T.J., McIntyre P., Bevan S. (2002) **A TRP Channel that Senses Cold Stimuli and Menthol** *Cell* **108**:705–715

5. McKemy D.D., Neuhausser W.M., D. and Julius (2002) **Identification of a cold receptor reveals a general role for TRP channels in thermosensation** *Nature* **416**:52–58

6. Škop Vojtěch, Guo Juen, Liu Naili, Xiao Cuiying, Hall Kevin D., Gavrilova Oksana, Reitman Marc L. (2020) **Mouse Thermoregulation: Introducing the Concept of the Thermoneutral Point** *Cell Reports* **31** https://doi.org/10.1016/j.celrep.2020.03.065

7. Yarmolinsky David A., Peng Yueqing, Pogorzala Leah A., Rutlin Michael, Hoon Mark A., Zuker Charles S. (2016) **Coding and Plasticity in the Mammalian Thermosensory System** *Neuron* https://doi.org/10.1016/j.neuron.2016.10.021

8. Tan Chan Lek, Cooke Elizabeth K., Leib David E., Lin Yen-Chu, Daly Gwendolyn E., Zimmerman Christo-pher A., Knight Zachary A. (2016) **Warm-Sensitive Neurons that Control Body Temperature** *Cell* https://doi.org/10.1016/j.cell.2016.08.028

9. Vilar Bruno, Tan Chun-Hsiang, McNaughton Peter A. (2020) **Heat detection by the TRPM2 ion channel** *Nature* **584**:E5–E12 https://doi.org/10.1038/s41586-020-2510-7

10. Mulier Marie, Vandewauw Ine, Vriens Joris, Voets Thomas (2020) **Reply to: Heat detection by the TRPM2 ion channel** *Nature* **584**:E13–E15 https://doi.org/10.1038/s41586-020-2511-6

11. Tominaga Makoto, Caterina Michael J., Malmberg Annika B., Rosen Tobias A., Gilbert Heather, Skinner Kate, Raumann Brigitte E., Basbaum Allan I., Julius David (1998) **The cloned capsaicin receptor integrates multiple pain-producing stimuli** *Neuron* **21**:531–543

12. Caterina M. J., Leffler A., Malmberg A. B., Martin W. J., Trafton J., Petersen-Zeitz K. R., Koltzenburg M., Basbaum A. I., Julius D. (2000) **Impaired Nociception and Pain Sensation in Mice Lacking the Capsaicin Receptor** *Science* **288**:306–313 https://doi.org/10.1126/science.288.5464.306

13. Davis John B. *et al.* (2000) **Vanilloid receptor-1 is essential for inflammatory thermal hyperalgesia** *Nature* **405**:183–187 https://doi.org/10.1038/35012076

14. Shimizu Isao, Iida Tohko, Guan Yun, Zhao Chengshui, Raja Srinivasa N., Jarvis Michael F., Cockayne Debra A., Caterina Michael J. (2005) **Enhanced thermal avoidance in mice lacking the ATP receptor P2X3** *Pain* **116**:96–108 https://doi.org/10.1016/j.pain.2005.03.030

15. Pogorzala L. A., Mishra S. K., Hoon M. A. (2013) **The Cellular Code for Mammalian Thermosensation** *Journal of Neuroscience* **33**:5533–5541 https://doi.org/10.1523/JNEUROSCI.5788-12.2013

16. Marics Irène, Malapert Pascale, Reynders Ana, Gaillard Stéphane, Moqrich Aziz (2014) **Acute Heat-Evoked Temperature Sensation Is Impaired but Not Abolished in Mice Lacking TRPV1 and TRPV3 Channels** *PLOS ONE* **9** https://doi.org/10.1371/journal.pone.0099828

17. Paricio-Montesinos Ricardo, Schwaller Frederick, Udhayachandran Annapoorani, Rau Florian, Walcher Jan, Evangelista Roberta, Vriens Joris, Voets Thomas, Poulet James F.A., Lewin Gary R. (2020) **The Sensory Coding of Warm Perception** *Neuron* https://doi.org/10.1016/j.neuron.2020.02.035

18. Togashi Kazuya, Hara Yuji, Tominaga Tomoko, Higashi Tomohiro, Konishi Yasunobu, Mori Yasuo, Tominaga Makoto (2006) **TRPM2 activation by cyclic ADP-ribose at body temperature is involved in insulin secretion** *The EMBO Journal* **25**:1804–1815 https://doi.org/10.1038/sj.emboj.7601083

19. Bartók Ádám, Csanády László (2022) **Dual amplification strategy turns TRPM2 channels into supersensitive central heat detectors** *Proceedings of the National Academy of Sciences* **119** https://doi.org/10.1073/pnas.2212378119

20. Ujisawa Tomoyo, Sasajima Sachiko, Kashio Makiko, Tominaga Makoto (2022) **Thermal gradient ring reveals different temperature-dependent behaviors in mice lacking thermosensitive TRP channels** *The Journal of Physiological Sciences* **72** https://doi.org/10.1186/s12576-022-00835-3

21. Wang Feng, Bélanger Erik, Côté Sylvain L., Desrosiers Patrick, Prescott Steven A., Côté Daniel C., De Koninck Yves (2018) **Sensory Afferents Use Different Coding Strategies for Heat and Cold** *Cell Reports* **23**:2001–2013 https://doi.org/10.1016/j.celrep.2018.04.065

22. Mota-Rojas Daniel, Titto Cristiane Gonçalves, Orihuela Agustín, Martínez-Burnes Julio, Gómez-Prado Jocelyn, Torres-Bernal Fabiola, Flores-Padilla Karla, Fuente Verónica Carvajal-de la, Wang Dehua (2021) **Physiological and Behavioral Mechanisms of Thermoregulation in Mammals** *Animals* **11** https://doi.org/10.3390/ani11061733

23. Gordon Christopher J, Becker Peggy, Ali Joseph S (1998) **Behavioral thermoregulatory responses of single- and group-housed mice** *Physiology & Behavior* **65**:255–262 https://doi.org/10.1016/S0031-9384(98)00148-6

24. Moqrich Aziz, Hwang Sun Wook, Earley Taryn J., Petrus Matt J., Murray Amber N., Spencer Kathryn S. R., Andahazy Mary, Story Gina M., Patapoutian Ardem (2005) **Impaired Thermosensation in Mice Lacking TRPV3, a Heat and Camphor Sensor in the Skin** *Science* **307**:1468–1472 https://doi.org/10.1126/science.1108609

25. Touska Filip, Winter Zoltán, Mueller Alexander, Vlachova Viktorie, Larsen Jonas, Zimmermann Katharina (2016) **Comprehensive thermal preference phenotyping in mice using a novel automated circular gradient assay** *Temperature* **3**:77–91 https://doi.org/10.1080/23328940.2015.1135689

26. Romanovsky A. A. (2014) **Skin temperature: Its role in thermoregulation** *Acta Physiologica* **210**:498–507 https://doi.org/10.1111/apha.12231

27. Tan Chun-Hsiang, McNaughton Peter A. (2016) **The TRPM2 ion channel is required for sensitivity to warmth** *Nature* **536**:460–463 https://doi.org/10.1038/nature19074

28. Mishra Santosh K, Tisel Sarah M, Orestes Peihan, Bhangoo Sonia K, Hoon Mark A (2011) **TRPV1-lineage neurons are required for thermal sensation** *The EMBO Journal* **30**:582–593 https://doi.org/10.1038/emboj.2010.325

29. Perner Caroline, Sokol Caroline L. (2021) **Protocol for dissection and culture of murine dorsal root ganglia neurons to study neuropeptide release** *STAR Protocols* **2** https://doi.org/10.1016/j.xpro.2021.100333

30. Leijon Sara C. M., Neves Amanda F., Breza Joseph M., Simon Sidney A., Chaudhari Nirupa, Roper Stephen D. (2019) **Oral thermosensing by murine trigeminal neurons: Modulation by capsaicin, menthol and mustard oil** *The Journal of Physiology* **597**:2045–2061 https://doi.org/10.1113/JP277385

31. Ono Kentaro (2012) **Comparison of the electrophysiological and immunohistochemical properties of acutely dissociated and 1-day cultured rat trigeminal ganglion neurons** *Neuroscience Letters*

32. Tsujino Hiroaki, Kondo Eiji, Fukuoka Tetsuo, Dai Yi, Tokunaga Atsushi, Miki Kenji, Yonenobu Kazuo, Ochi Takahiro, Noguchi Koichi (2000) **Activating Transcription Factor 3 (ATF3) Induction by Axotomy in Sensory and Motoneurons: A Novel Neuronal Marker of Nerve Injury** *Molecular and Cellular Neuroscience* **15**:170–182 https://doi.org/10.1006/mcne.1999.0814

33. Zheng Ji-Hong, Walters Edgar T., Song Xue-Jun (2007) **Dissociation of Dorsal Root Ganglion Neurons Induces Hyperexcitability That Is Maintained by Increased Responsiveness to cAMP and cGMP** *Journal of Neurophysiology* **97**:15–25 https://doi.org/10.1152/jn.00559.2006

34. Huang Zhi-Jiang, Li Hao-Chuan, Cowan Ashley A., Liu Su, Zhang Yan-Kai, Song Xue-Jun (2012) **Chronic compression or acute dissociation of dorsal root ganglion induces cAMP-dependent neuronal hyperexcitability through activation of PAR2** *PAIN* **153**:1426–1437 https://doi.org/10.1016/j.pain.2012.03.025

35. Wangzhou Andi *et al.* (2020) **Pharmacological target-focused transcriptomic analysis of native vs cultured human and mouse dorsal root ganglia** *Pain* **161**:1497–1517 https://doi.org/10.1097/j.pain.0000000000001866

36. Nguyen Minh Q, Le Pichon Claire E, Ryba Nicholas (2019) **Stereotyped transcriptomic transformation of somatosensory neurons in response to injury** *eLife* **8** https://doi.org/10.7554/eLife.49679

37. Hanack Christina *et al.* (2015) **GABA Blocks Pathological but Not Acute TRPV1 Pain Signals** *Cell* **160**:759–770 https://doi.org/10.1016/j.cell.2015.01.022

38. Lebovich Lior, Yunerman Michael, Scaiewicz Viviana, Loewenstein Yonatan, Rokni Dan (2021) **Paradoxical relationship between speed and accuracy in olfactory figure-background segregation** *PLOS Computational Biology* **17** https://doi.org/10.1371/journal.pcbi.1009674

39. Hanks Timothy D., Kopec Charles D., Brunton Bingni W., Duan Chunyu A., Erlich Jeffrey C., Brody Carlos D. (2015) **Distinct relationships of parietal and prefrontal cortices to evidence accumulation** *Nature* **520**:220–223 https://doi.org/10.1038/nature14066

40. Stine Gabriel M., Trautmann Eric M., Jeurissen Danique, Shadlen Michael N. (2023) **A neural mechanism for terminating decisions** *Neuron* **111**:2601–2613 https://doi.org/10.1016/j.neuron.2023.05.028

41. Deco Gustavo, Rolls Edmund T., Albantakis Larissa, Romo Ranulfo (2013) **Brain mechanisms for perceptual and reward-related decision-making** *Progress in Neurobiology* **103**:194–213 https://doi.org/10.1016/j.pneurobio.2012.01.010

42. Gupta Ankur, Bansal Rohini, Alashwal Hany, Kacar Anil Safak, Balci Fuat, Moustafa Ahmed A. (2022) **Neural Substrates of the Drift-Diffusion Model in Brain Disorders** *Frontiers in Computational Neuroscience* **15**

43. Vandewauw Ine *et al.* (2018) **A TRP channel trio mediates acute noxious heat sensing** *Nature* https://doi.org/10.1038/nature26137

44. Ratcliff Roger (1978) **A theory of memory retrieval** *Psychological Review* **85**:59–108 https://doi.org/10.1037/0033-295X.85.2.59

45. Renthal William, Tochitsky Ivan, Yang Lite, Cheng Yung-Chih, Li Emmy, Kawaguchi Riki, Geschwind Daniel H., Woolf Clifford J. (2020) **Transcriptional Reprogramming of Distinct Peripheral Sensory Neuron Subtypes after Axonal Injury** *Neuron* https://doi.org/10.1016/j.neuron.2020.07.026

46. Sharma Nikhil, Flaherty Kali, Lezgiyeva Karina, Wagner Daniel E., Klein Allon M., Ginty David D. (2020) **The emergence of transcriptional identity in somatosensory neurons** *Nature* https://doi.org/10.1038/s41586-019-1900-1

47. Qi Lijun *et al.* (2023) **A DRG genetic toolkit reveals molecular, morphological, and functional diversity of somatosensory neuron subtypes** *bioRxiv* https://doi.org/10.1101/2023.04.22.537932

48. Marmigère F., P. and Ernfors (2007) **Specification and connectivity of neuronal subtypes in the sensory lineage** *Nat. Rev. Neurosci* **8**:114–127

49. Wu Haohao *et al.* (2021) **Distinct subtypes of proprioceptive dorsal root ganglion neurons regulate adaptive proprioception in mice** *Nature Communications* **12** https://doi.org/10.1038/s41467-021-21173-9

50. Choi Seungwon *et al.* (2020) **Parallel ascending spinal pathways for affective touch and pain** *Nature* **587**:258–263 https://doi.org/10.1038/s41586-020-2860-1

51. Morrison S.F., Nakamura K. (2019) **Central Mechanisms for Thermoregulation** *Annual Review of Physiology* **81**:285–308 https://doi.org/10.1146/annurev-physiol-020518-114546

52. Song K., Wang H., Kamm G. B., Pohle J., Reis F. d. C., Heppenstall P., Wende H., Siemens J. (2016) **The TRPM2 channel is a hypothalamic heat sensor that limits fever and can drive hypothermia** *Science* **353**:1393–1398 https://doi.org/10.1126/science.aaf7537

53. Kamm Gretel B. *et al.* (2021) **A synaptic temperature sensor for body cooling** *Neuron* **109**:3283–3297 https://doi.org/10.1016/j.neuron.2021.10.001

54. Yang Yaoheng *et al.* (2023) **Induction of a torpor-like hypothermic and hypometabolic state in rodents by ultrasound** *Nature Metabolism* **5** https://doi.org/10.1038/s42255-023-00804-z

55. Mathis Alexander, Mamidanna Pranav, Cury Kevin M., Abe Taiga, Murthy Venkatesh N., Mathis Mackenzie Weygandt, Bethge Matthias (2018) **DeepLabCut: Markerless pose estimation of user-defined body parts with deep learning** *Nature Neuroscience* **21**:1281–1289 https://doi.org/10.1038/s41593-018-0209-y

56. Pachitariu Marius, Stringer Carsen, Schröder Sylvia, Dipoppa Mario, Rossi L. Federico, Carandini Matteo, Harris Kenneth D. (2016) **Suite2p: Beyond 10,000 neurons with standard two-photon microscopy** *bioRxiv* https://doi.org/10.1101/061507

57. Stringer Carsen, Wang Tim, Michaelos Michalis, Pachitariu Marius (2021) **Cellpose: A generalist algorithm for cellular segmentation** *Nature Methods* **18**:100–106 https://doi.org/10.1038/s41592-020-01018-x

58. Oliver Ann E., Baker Gary A., Fugate Robert D., Tablin Fern, Crowe John H. (2000) **Effects of Temperature on Calcium-Sensitive Fluorescent Probes** *Biophysical Journal* **78**:2116–2126 https://doi.org/10.1016/S0006-3495(00)76758-0

59. Dempster Angus, Schmidt Daniel F., Webb Geoffrey I. (2021) **MINIROCKET: A Very Fast (Almost) Deterministic Transform for Time Series Classification** *In Proceedings of the 27th ACM SIGKDD Conference on Knowledge Discovery & Data Mining* :248–257 https://doi.org/10.1145/3447548.3467231

60. Vehtari Aki, Gelman Andrew, Gabry Jonah (2017) **Practical Bayesian model evaluation using leave-one-out cross-validation and WAIC** *Statistics and Computing* **27**:1413–1432 https://doi.org/10.1007/s11222-016-9696-4

Article and author information

Muad Y. Abd El Hay
Department of Pharmacology, Heidelberg University, Heidelberg, Germany, Ernst Strüngmann Institute for Neuroscience in cooperation with the Max Planck Society, Frankfurt am Main, 60528, Germany
For correspondence: muad.abdelhay@gmail.com
ORCID iD: 0000-0002-5082-1216

Gretel B. Kamm
Department of Pharmacology, Heidelberg University, Heidelberg, Germany
ORCID iD: 0000-0002-2630-2010

Alejandro Tlaie
Ernst Strüngmann Institute for Neuroscience in cooperation with the Max Planck Society, Frankfurt am Main, 60528, Germany, Laboratory for Clinical Neuroscience, Centre for Biomedical Technology, Technical University of Madrid, Spain
ORCID iD: 0000-0002-6844-5765

Jan Siemens
Department of Pharmacology, Heidelberg University, Heidelberg, Germany
For correspondence: jan.siemens@pharma.uni-heidelberg.de
ORCID iD: 0000-0002-3431-2665

Editors

Reviewing Editor
Andres Jara-Oseguera
The University of Texas at Austin, Austin TX, United States of America

Senior Editor
Kenton Swartz
National Institute of Neurological Disorders and Stroke, National Institutes of Health, Bethesda, United States of America

Reviewer #1 (Public Review):

Summary:

The authors use an innovative behavior assay (chamber preference test) and standard calcium imaging experiments on cultured dorsal root ganglion (DRG) neurons to evaluate the consequences of global knockout of TRPV1 and TRPM2, and overexpression of TRPV1, on warmth detection. They find a profound effect of TRPM2 elimination in the behavioral assay, whereas elimination of TRPV1 has the largest effect on neuronal responses. These findings are of importance, as there is still substantial discussion in the field regarding the contribution of TRP channels to different aspects of thermosensation.

Strengths:

The chamber preference test is an important innovation compared to the standard two-plate test, as it depends on thermal information sampled from the entire skin, as opposed to only the plantar side of the paws. With this assay, and the detailed analysis, the authors provide strong supporting evidence for the role of TRPM2 in warmth avoidance. The conceptual framework using the Drift Diffusion Model provides a first glimpse of how this decision of a mouse to change between temperatures can be interpreted and may form the basis for further analysis of thermosensory behavior.

Weaknesses:

The authors juxtapose these behavioral data with calcium imaging data using isolated DRG neurons. Here, there are a few aspects that are less convincing.

(1) The authors study warmth responses using DRG neurons after three days of culturing. They propose that these "more accurately reflect the functional properties and abundance of warm-responsive sensory neurons that are found in behaving animals." However, the only argument to support this notion is that the fraction of neurons responding to warmth is lower after three days of culture. This could have many reasons, including loss of specific subpopulations of neurons, or any other (artificial?) alterations to the neurons' transcriptome due to the culturing. The isolated DRGs are not selected in any way, so also include neurons innervating viscera not involved in thermosensation. If the authors wish to address actual changes in sensory nerves involved in warmth sensing in TRPM2 or TRPV1 KO mice without

disturbing the response profile as a result of the isolation procedure, other approaches would be needed (e.g. skin-nerve recordings or in vivo DRG imaging).

(2) The authors state that there is a reduction in warmth-sensitive DRG neurons in the TRPM2 knockout mice based on the data presented in Figure 2D. This is not convincing for the following reasons. First, the authors used t-tests (with FDR correction - yielding borderline significance) whereas three groups are compared here in three repetitive stimuli. This would require different statistics (e.g. ANOVA), and I am not convinced (based on a rapid assessment of the data) that such an analysis would yield any significant difference between WT and TRPM2 KO. Second, there seems to be a discrepancy between the plot and legend regarding the number of LOV analysed (21, 17, and 18 FOV according to the legend, compared to 18, 10, and 12 dots in the plot). Therefore, I would urge the authors to critically assess this part of the study and to reconsider whether the statement (and discussion) that "Trpm2 deletion reduces the proportion of warmth responders" should be maintained or abandoned.

(3) It remains unclear whether the clear behavioral effect seen in the TRPM2 knockout animals is at all related to TRPM2 functioning as a warmth sensor in sensory neurons. As discussed above, the effects of the TRPM2 KO on the proportion of warmth-sensing neurons are at most very subtle, and the authors did not use any pharmacological tool (in contrast to the use of capsaicin to probe for TRPV1 in Figures S3 and S4) to support a direct involvement of TRPM2 in the neuronal warmth responses. Behavioral experiments on sensory-neuron-specific TRPM2 knockout animals will be required to clarify this important point.

(4) The authors only use male mice, which is a significant limitation, especially considering known differences in warmth sensing between male and female animals and humans. The authors state "For this study, only male animals were used, as we aimed to compare our results with previous studies which exclusively used male animals (7, 8, 17, 43)." This statement is not correct: all four mentioned papers include behavioral data from both male and female mice! I recommend the authors to either include data from female mice or to clearly state that their study (in comparison with these other studies) only uses male mice.

https://doi.org/10.7554/eLife.95618.1.sa2

Reviewer #2 (Public Review):

Summary:

The authors of the study use a technically well-thought-out approach to dissect the question of how far TRPV1 and TRPM2 are involved in the perception of warm temperatures in mice. They supplement the experimental data with a drift-diffusion model. They find that TRPM2 is required to trigger the preference for 31{degree sign}C over warmer temperatures while TRPV1 increases the fidelity of afferent temperature information. A lack of either channel leads to a depletion of warm-sensing neurons and in the case of TRPV1 to a deficit in rapid responses to temperature changes. The study demonstrates that mouse phenotyping can only produce trustworthy results if the tools used to test them measure what we believe they are measuring.

Strengths:

The authors tackle a central question in physiology to which we have not yet found sufficient answers. They take a pragmatic approach by putting existing experimental methods to the test and refining them significantly.

Weaknesses:

It is difficult to find weaknesses. Not only the experimental methods but also the data analysis have been refined meticulously. There is no doubt that the authors achieved their aims and that the results support their conclusions.

There will certainly be some lasting impact on the future use of DRG cultures with respect to (I) the incubation periods, (II) how these data need to be analyzed, and (III) the numbers of neurons to be looked at.

As for the CPT assay, the future will have to show if mouse phenotyping results are more accurate with this technique. I'm more fond of full thermal gradient environments. However, behavioural phenotyping is still one of the most difficult fields in somatosensory research.

https://doi.org/10.7554/eLife.95618.1.sa1

Reviewer #3 (Public Review):

Summary and strengths:

In the manuscript, Abd El Hay et al investigate the role of thermally sensitive ion channels TRPM2 and TRPV1 in warm preference and their dynamic response features to thermal stimulation. They develop a novel thermal preference task, where both the floor and air temperature are controlled, and conclude that mice likely integrate floor with air temperature to form a thermal preference. They go on to use knockout mice and show that TRPM2-/- mice play a role in the avoidance of warmer temperatures. Using a new approach for culturing DRG neurons they show the involvement of both channels in warm responsiveness and dynamics. This is an interesting study with novel methods that generate important new information on the different roles of TRPV1 and TRPM2 on thermal behavior.

Open questions and weaknesses:

(1) Differences in the response features of cells expressing TRPM2 and TRPV1 are central and interesting findings but need further validation (Figures 3 and 4). To show differences in the dynamics and the amplitude of responses across different lines and stimulus amplitudes more clearly, the authors should show the grand average population calcium response from all responsive neurons with error bars for all 3 groups for the different amplitudes of stimuli (as has been presented for the thermal stimuli traces). The authors should also provide a population analysis of the amplitude of the responses in all groups to all stimulus amplitudes. Prior work suggests that thermal detection is supported by an enhancement or suppression of the ongoing activity of sensory fibers innervating the skin. The authors should present any data on cells with ongoing activity.

(2) The authors should better place their findings in context with the literature and highlight the novelty of their findings. The introduction builds a story of a 'disconnect' or 'contradictory' findings about the role of TRPV1 and TRPM2 in warm detection. While there are some disparate findings in the literature, Tan and McNaughton (2016) show a role for TRPM2 in the avoidance of warmth in a similar task, Paricio et al. (2020) show a significant reduction in warm perception in TRPM2 and TRPV1 knock out lines and Yarmolinksy et al. (2016) show a reduction in warm perception with TRPV1 inactivation. All these papers are therefore in agreement with the authors finding of a role for these channels in warm behavior. The authors should change their introduction and discussion to more correctly discuss the findings of these studies and to better pinpoint the novelty of their own work.

(3) The responses of 60 randomly selected cells are shown in Figure 2B. But, looking at the TRPM2-/- data, warm responses appear more obvious than in WTs and the weaker responders of the WT group appear weaker than the equivalent group in the TRPV1-/- and

TRPM2-/- data. This does not necessarily invalidate the results, but it may suggest a problem in the data selection. Because the correct classification of warm-sensitive neurons is central to this part of the study more validation of the classifier should be presented. For example, the authors could state if they trained the classifier using equal amounts of cells, show some randomly selected cells that are warm-insensitive for all genotypes, and show the population average responses of warm-insensitive neurons.

(4) The interpretation of the main behavioral results and justification of the last figure is presented as the result of changes in sensing but differences in this behavior could be due to many factors and this needs clarification and discussion. (i) The authors mention that 'crucially temperature perception is not static' and suggest that there are fluctuating changes in perception over time and conclude that their modelling approach helps show changes in temperature detection. They imply that temperature perceptual threshold changes over time, but the mouse could just as easily have had exactly the same threshold throughout the task but their motivation (or some other cognitive variable) might vary causing them to change chamber. The authors should correct this. (ii) Likewise, from their fascinating and high-profile prior work the authors suggest a model of internal temperature sensing whereby TRPM2 expression in the hypothalamus acts as an internal sensory of body temperature. Given this, and the slow time course of the behavior in chambers with different ambient temperatures, couldn't the reason for the behavioral differences be due to central changes in hypothalamic processing rather than detection by skin temperature? If TRPM2-/- were selectively ablated from the skin or the hypothalamus (these experiments are not necessary for this paper) it might be possible to conclude whether sensation or body temperature is more likely the root cause of these effects but, without further experiments it is tough to conclude either way. (iii) Because the ambient temperature is controlled in this behavior, another hypothesis is that warm avoidance could be due to negative valence associated with breathing warm air, i.e. a result of sensation within the body in internal pathways, rather than sensing from the external skin. Overall, the authors should tone down conclusions about sensation and present a more detailed discussion of these points.

(5) It is an excellent idea to present a more in-depth analysis of the behavioral data collected during the preference task, beyond 'the mouse is on one side or the other'. However, the drift-diffusion approach is complex to interpret from the text in the results and the figures. The results text is not completely clear on which behavioral parameters are analyzed and terms like drift, noise, estimate, and evidence are not clearly defined. Currently, this section of the paper slightly confuses and takes the paper away from the central findings about dynamics and behavioral differences. It seems like they could come to similar conclusions with simpler analysis and simpler figures.

(6) In Figure 2D the % of warm-sensitive neurons are shown for each genotype. Each data point is a field of view, however, reading the figure legend there appear to be more FOVs than data points (eg 10 data points for the TRPV1-/- but 17 FOVs). The authors should check this.

(7) Can the authors comment on why animals with over-expression of TRPV1 spend more time in the warmest chamber to start with at 38C and not at 34C?

https://doi.org/10.7554/eLife.95618.1.sa0

Author Response:

> ***Reviewer #1:***
>
> *Summary:*

> *The authors use an innovative behavior assay (chamber preference test) and standard calcium imaging experiments on cultured dorsal root ganglion (DRG) neurons to evaluate the consequences of global knockout of TRPV1 and TRPM2, and overexpression of TRPV1, on warmth detection. They find a profound effect of TRPM2 elimination in the behavioral assay, whereas elimination of TRPV1 has the largest effect on neuronal responses. These findings are of importance, as there is still substantial discussion in the field regarding the contribution of TRP channels to different aspects of thermosensation.*
>
> *Strengths:*
>
> *The chamber preference test is an important innovation compared to the standard two-plate test, as it depends on thermal information sampled from the entire skin, as opposed to only the plantar side of the paws. With this assay, and the detailed analysis, the authors provide strong supporting evidence for the role of TRPM2 in warmth avoidance. The conceptual framework using the Drift Diffusion Model provides a first glimpse of how this decision of a mouse to change between temperatures can be interpreted and may form the basis for further analysis of thermosensory behavior.*
>
> *Weaknesses:*
>
> *The authors juxtapose these behavioral data with calcium imaging data using isolated DRG neurons. Here, there are a few aspects that are less convincing.*
>
> *(1) The authors study warmth responses using DRG neurons after three days of culturing. They propose that these "more accurately reflect the functional properties and abundance of warm-responsive sensory neurons that are found in behaving animals." However, the only argument to support this notion is that the fraction of neurons responding to warmth is lower after three days of culture. This could have many reasons, including loss of specific subpopulations of neurons, or any other (artificial?) alterations to the neurons' transcriptome due to the culturing. The isolated DRGs are not selected in any way, so also include neurons innervating viscera not involved in thermosensation. If the authors wish to address actual changes in sensory nerves involved in warmth sensing in TRPM2 or TRPV1 KO mice without disturbing the response profile as a result of the isolation procedure, other approaches would be needed (e.g. skin-nerve recordings or in vivo DRG imaging).*

We agree that there could be several reasons as to why the responses of cultured DRGs are reduced compared to the acute/short-term cultures. It is possible —and likely— that

transcriptional changes happen over the course of the culturing period. It is also possible that it is a mere coincidence that the 3-day cultures have a response profile more similar to the in vivo situation than the acute cultures. In the revised manuscript, we will therefore tone down the claim that the 3-day cultures mirror the native conditions more appropriately.

Nevertheless, our results clearly show that acute cultures have a response profile that is much more similar to damaged/”inflamed” neurons, irrespective of any comparison to the 3 daycultures. Therefore, we believe, it is helpful to include this data to make scientists aware that acute cultures are very different to non-inflamed native/in vivo DRG neurons that many researchers use in their experiments.

In some experiments not shown in the first version of our manuscript, we applied the TRPchannel agonists Menthol, Capsaicin and AITC (mustard oil) consecutively in a few 3-day

cultures. We also have Capsaicin responses from overnight cultures. We will attempt to correlate the percentage of the neurons responsive to these TRPV1, TRPM8 and TRPA1

ion channel agonists in our cultures to the percentages of neurons found to express the respective TRP ion channels (TRPM8, TRPV1 and TRPA1) in vivo. While this type of

analysis won't prove that 3-day cultures are similar to the in vivo situation (even if there is good correlation between the in vitro and in vivo results), it might support the usage of 3-day cultures as a model.

> *(2) The authors state that there is a reduction in warmth-sensitive DRG neurons in the TRPM2 knockout mice based on the data presented in Figure 2D. This is not convincing for the following reasons. First, the authors used t-tests (with FDR correction - yielding borderline significance) whereas three groups are compared here in three repetitive stimuli. This would require different statistics (e.g. ANOVA), and I am not convinced (based on a rapid assessment of the data) that such an analysis would yield any significant difference between WT and TRPM2 KO. Second, there seems to be a discrepancy between the plot and legend regarding the number of LOV analysed (21, 17, and 18 FOV according to the legend, compared to 18, 10, and 12 dots in the plot). Therefore, I would urge the authors to critically assess this part of the study and to reconsider whether the statement (and discussion) that "Trpm2 deletion reduces the proportion of warmth responders" should be maintained or abandoned.*

Yes, we agree that the statistical tests indicated by the referee are more appropriate/robust for the data shown in Figures 1F, 2D, and 4G.

When we perform 2-way repeated measures ANOVA and subsequent multiple comparison test (with Dunnets correction) against Wildtype, for data shown in Fig. 2D, both the main effect (Genotype) and the interaction term (Stimulus x Genotype) are significant. The multiple comparison yields very similar result as in the current manuscript, with the difference that the TRPM2-KO data for the 2nd stimulus (~36°C) is borderline significant (with a p-value of p=0.050).

Due to the possible dependence of the repeated temperature stimuli and the variability of each stimulus between FOVs (Fig. 2C), it is possible that a mixed-effect model that accounts for these effects is more appropriate.

Similarly, for plots 1F and 4G, Genotype (either as main effect or as interaction with Time) is significant after a repeated measures two-way ANOVA. The multiple comparisons (with Bonferroni correction) only changed the results marginally at individual timepoints, without affecting the overall conclusions. The exception is Fig. 4G at 38°C, where the interaction of Time and Genotype is significant, but no individual timepoint-comparison is significant after Bonferroni correction.

The main difference between the results presented above and the ones presented in the manuscript is the choice of the multiple comparison correction. We originally opted for the falsediscovery rate (FDR) approach as it is less prone to Type II errors (false negatives) than other methods such as Sidaks or Bonferroni, particularly when correcting for a large number of tests. However, we are mainly interested in whether the genotypes differ in their behavior in each temperature combination and the significant ANOVA tests for Fig. 1F and 4G support that point. The statistical test and comparison used in the current version of the manuscript, comparing behavior at individual/distinct timepoints, are interesting, but less relevant (and potentially distracting), as we do not go into the details about the behavior at any given/distinct timepoint in the assay.

Therefore, and per suggestion of the reviewer, we will update the statistics in the revised version of the manuscript. Also, we will report the correct number of FOVs in the legend.

> *(3) It remains unclear whether the clear behavioral effect seen in the TRPM2 knockout animals is at all related to TRPM2 functioning as a warmth sensor in sensory neurons. As discussed above, the effects of the TRPM2 KO on the proportion of warmth-sensing neurons are at most very subtle, and the authors did not use any pharmacological tool (in contrast to the use of capsaicin to probe for TRPV1 in Figures S3 and S4) to support a direct involvement of TRPM2 in the neuronal warmth responses. Behavioral experiments on sensory-neuron-specific TRPM2 knockout animals will be required to clarify this important point.*

As mentioned above, we will tone down the correlation between the cellular and behavioral data and further stress the possibility that the Trpm2-KO phenotype is possibly related to the function of the ion channel outside of DRGs.

> *(4) The authors only use male mice, which is a significant limitation, especially considering known differences in warmth sensing between male and female animals and humans. The authors state "For this study, only male animals were used, as we aimed to compare our results with previous studies which exclusively used male animals (7, 8, 17, 43)." This statement is not correct: all four mentioned papers include behavioral data from both male and female mice! I recommend the authors to either include data from female mice or to clearly state that their study (in comparison with these other studies) only uses male mice.*

In the studies by Tan et al. And Vandevauw et al. Only male animals were used for the behavioral experiments. Yarmolinsky et al. And Paricio-Montesinons et al. used both males and females while, as far as we can tell, only Paricio-Montesions et al. Reported that no difference was observed between the sexes. This is a valid point though -- when our study started 6-7 years ago, we only used male mice (as did many other researchers) and this we would now do differently. Nevertheless, we included some female mice in these experiments and will reevaluate if the numbers are sufficient so that we can generalize the phenotypes to both sexes or report differences in the revised ms.

Wildtypes are all C57bl/6N from the provider Janvier. Generally, all lines are backcrossed to C57bl/6 mice and additionally inbreeding was altered every 4-6 generations by crossing to C57bl/6. Exactly how many times the Trp channel KOs have been backcrossed to C57bl/6 mice we cannot exactly state.

> ***Reviewer #3:***
>
> *Summary and strengths:*
>
> *In the manuscript, Abd El Hay et al investigate the role of thermally sensitive ion channels TRPM2 and TRPV1 in warm preference and their dynamic response features to thermal stimulation. They develop a novel thermal preference task, where both the floor and air temperature are controlled, and conclude that mice likely integrate floor with air temperature to form a thermal preference. They go on to use knockout mice and show that TRPM2-/- mice play a role in the avoidance of warmer temperatures. Using a new approach for culturing DRG neurons they show the involvement of both channels in warm responsiveness and dynamics. This is an interesting study with novel methods that generate important new information on the different roles of TRPV1 and TRPM2 on thermal behavior.*
>
> *Open questions and weaknesses:*
>
> *(1) Differences in the response features of cells expressing TRPM2 and TRPV1 are central and interesting findings but need further validation (Figures 3 and 4). To show*

> *differences in the dynamics and the amplitude of responses across different lines and stimulus amplitudes more clearly, the authors should show the grand average population calcium response from all responsive neurons with error bars for all 3 groups for the different amplitudes of stimuli (as has been presented for the thermal stimuli traces). The authors should also provide a population analysis of the amplitude of the responses in all groups to all stimulus amplitudes. Prior work suggests that thermal detection is supported by an enhancement or suppression of the ongoing activity of sensory fibers innervating the skin. The authors should present any data on cells with ongoing activity.*

We will include grand average population analysis of the different groups in the revised version.

Concerning the point about ongoing activity: We are not sure if it is possible in neuronal cultures to faithfully recapitulate ongoing activity. Ongoing activity has been mostly recorded in skinnerve preparations (or in older studies in other types of nerve recordings) and there are only very few studies that show ongoing activity in cultured experiments and then the ongoing activity only starts in sensory neuron cultures when cultured for even longer time periods than 3 days (Ref.: doi: 10.1152/jn.00158.2018). We have very few cells that show some spontaneous activity, but these are too few to draw any conclusions. In any case, nerve fibers might be necessary to drive ongoing activity which are absent from our cultures.

> *(2) The authors should better place their findings in context with the literature and highlight the novelty of their findings. The introduction builds a story of a 'disconnect' or 'contradictory' findings about the role of TRPV1 and TRPM2 in warm detection. While there are some disparate findings in the literature, Tan and McNaughton (2016) show a role for TRPM2 in the avoidance of warmth in a similar task, Paricio et al. (2020) show a significant reduction in warm perception in TRPM2 and TRPV1 knock out lines and Yarmolinksy et al. (2016) show a reduction in warm perception with TRPV1 inactivation. All these papers are therefore in agreement with the authors finding of a role for these channels in warm behavior. The authors should change their introduction and discussion to more correctly discuss the findings of these studies and to better pinpoint the novelty of their own work.*

Paricio-Montesinos et al. argue that TRPM8 is crucial for the detection of warmth, as TRPM8-KO animals are incapable of learning the operant task. TRPM2-KO animals and, to a smaller extent TRPV1-KO animals, have reduced sensitivity in the task, but are still capable of learning/performing the task. However, in our chamber preference assay this is reversed: TRPM2-KO animals lose the ability to differentiate warm temperatures while TRPM8 appears to play no major role. A commonality between the two studies is that while TRPV1 affects the detection of warm temperatures in the different assays, this ion channel appears not to be crucial.

Similarly, Yarmolinsky et al. show that Trpv1-inactivation only increases the error rate in their operant assay (from ~10% to ~30%), without testing TRPM2. And Tan et al. show the

importance of TRPM2 in the preference task, without testing for TRPV1.

More generally, the choice of the assay, being either an operant task (Paricio-Montesinos et al. and Yarmolinsky et al.) or a preference assay without training of the mice (Tan et al. and our data here), might be important and different TRP receptors may be relevant for different types of temperature assays, which we will extend on in the discussion in the revised manuscript. While our results generally agree with the previous studies, they add a different perspective on the analysis of the behavior (with correlation to cellular data). We will adjust the manuscript to highlight the advances more clearly.

> *(3) The responses of 60 randomly selected cells are shown in Figure 2B. But, looking at the TRPM2-/- data, warm responses appear more obvious than in WTs and the weaker responders of the WT group appear weaker than the equivalent group in the TRPV1-/- and TRPM2-/- data. This does not necessarily invalidate the results, but it may suggest a problem in the data selection. Because the correct classification of warm-sensitive neurons is central to this part of the study more validation of the classifier should be presented. For example, the authors could state if they trained the classifier using equal amounts of cells, show some randomly selected cells that are warm-insensitive for all genotypes, and show the population average responses of warm-insensitive neurons.*

The classifier was trained on a balanced dataset of 1000 (500 responders and 500 nonresponders), manually labelled traces across all 5 temperature stimuli. The prediction accuracy was 98%. We will describe more clearly how the classifier was trained and include examples and also show the population average responses in the revised manuscript.

> *(4) The interpretation of the main behavioral results and justification of the last figure is presented as the result of changes in sensing but differences in this behavior could be due to many factors and this needs clarification and discussion. (i) The authors mention that 'crucially temperature perception is not static' and suggest that there are fluctuating changes in perception over time and conclude that their modelling approach helps show changes in temperature detection. They imply that temperature perceptual threshold changes over time, but the mouse could just as easily have had exactly the same threshold throughout the task but their motivation (or some other cognitive variable) might vary causing them to change chamber. The authors should correct this. (ii) Likewise, from their fascinating and high-profile prior work the authors suggest a model of internal temperature sensing whereby TRPM2 expression in the hypothalamus acts as an internal sensory of body temperature. Given this, and the slow time course of the behavior in chambers with different ambient temperatures, couldn't the reason for the behavioral differences be due to central changes in hypothalamic processing rather than detection by skin temperature? If TRPM2-/- were selectively ablated from the skin or the hypothalamus (these experiments are not necessary for this paper) it might be possible to conclude whether sensation or body temperature is more likely the root cause of these effects but, without further experiments it is tough to conclude either way. (iii) Because the ambient temperature is controlled in this behavior, another hypothesis is that warm avoidance could be due to negative valence associated with breathing warm air, i.e. a result of sensation within the body in internal pathways, rather than sensing from the external skin. Overall, the authors should tone down conclusions about sensation and present a more detailed discussion of these points.*

We are sorry that the statement including the phrase “crucially temperature perception is not static” is ambiguous; what we meant to say is that with the mouse moving across the two chambers, the animal experiences different temperatures over time (not that the perceptual threshold of the mouse changes). We will clarify this stament in the revised version of the manuscript.

But even so, it could be that some other variable (motivation etc) makes the mouse change the chamber; we hypothesize that this variable (whatever it might be) is still modulated by temperature (at least this would be the likeliest explanation that we see).

As for the aspect of internal/hypothalamic temperature sensing: we have included this possibility already in the discussion but will further emphasize this possibility in the revised manuscript.

As for the point of negative valence mediated by breathing in warm air: yes, presumably this could also be possible. The aspect of valence is in interesting aspect by itself: would the mice be rather repelled from the (uncomfortable) hot plate or more attracted to the (more comfortable) thermoneutral plate, or both? Something to elucidate in a different study.

> *(5) It is an excellent idea to present a more in-depth analysis of the behavioral data collected during the preference task, beyond 'the mouse is on one side or the other'. However, the drift-diffusion approach is complex to interpret from the text in the results and the figures. The results text is not completely clear on which behavioral parameters are analyzed and terms like drift, noise, estimate, and evidence are not clearly defined. Currently, this section of the paper slightly confuses and takes the paper away from the central findings about dynamics and behavioral differences. It seems like they could come to similar conclusions with simpler analysis and simpler figures.*

We will reassess the description of the drift diffusion model and explain it more clearly. Additionally, we will assess whether we can introduce the drift diffusion model and analysis better at the beginning of the study, subsequent to Figure 1 to have the model and this type of analysis coherent with the first behavior results (instead of introducing the model only at the very end).

> *(6) In Figure 2D the % of warm-sensitive neurons are shown for each genotype. Each data point is a field of view, however, reading the figure legend there appear to be more FOVs than data points (eg 10 data points for the TRPV1-/- but 17 FOVs). The authors should check this.*

We check and make sure that in the revised manuscript the number of FOVs mentioned in the legend and the number shown in the Figure 2D are in agreement.

> *(7) Can the authors comment on why animals with over-expression of TRPV1 spend more time in the warmest chamber to start with at 38C and not at 34C?*

This is an interesting observation that we did not consider before. A closer look at Figure 4H reveals that the majority of the TRPV1-OX animals, have a proportionally long first visit to the 38°C room. We can only speculate why this is the case. We cannot rule out that this a technical shortcoming of the assay and how we conduced it – but we don't observe this for the wildtype mice, thus it is rather unlikely a technical problem. It is possible that this is a type of "freezing-" (or "startle-") behavior when the animals first encounter the 38°C temperature. Freezing behaviors in mice can be observed when sudden/threatening stimuli are applied. It is possible that, in the TRPV1-overexpressing animals, the initial encounter with 38°C leads to activation of a larger proportion of cells (compared to WT ctrls), possibly signaling a "painful" stimulus, and thus leading to this startle effect. It is noteworthy, however, that with more stringent repeated measure statistics applied as suggested by the referees, the difference at the first measured time point in Fig. 4G is not significantly different anymore (see comment #2 above. This does not rule out that this might be a true effect, but such a claim would benefit from additional experiments that test such and hypothesis more rigorously.